

Self-organization and time-stability of social hierarchies

Joseph Hickey* and Jörn Davidsen

Complexity Science Group
Department of Physics and Astronomy
University of Calgary

Abstract

The formation and stability of social hierarchies is a question of general relevance. Here, we propose a simple model for establishing social hierarchy via pair-wise interactions between individuals and investigate its stability. In each interaction or fight, the probability of “winning” depends solely on the relative societal status of the participants, and the winner has a gain of status whereas there is an equal loss to the loser. The interactions are characterized by two parameters. The first parameter represents how much can be lost, and the second parameter represents the degree to which even a small difference of status can guarantee a win for the higher-status individual. Depending on the parameters, the resulting status distributions reach either a continuous unimodal form or lead to a totalitarian end state with one dominant high-status individual and all other individuals having zero status. However, we find that in the latter case long-lived intermediary distributions often exist, which can give the illusion of a stable society. Moreover, by implementing a simple, but realistic rule that restricts interactions to sufficiently similar-status individuals, the stable or long-lived distributions acquire high-status structure corresponding to a dominant class. We compare our model predictions to human societies using household income as a proxy for societal status and find agreement over their entire range from the low-to-middle-status parts to the characteristic high-status “tail”. We discuss how the model provides a conceptual framework for understanding the origin of social hierarchy and the factors which lead to the preservation or deterioration of the societal structure.

*joseph.hickey@ucalgary.ca

1 Introduction

Animals, including humans, form social hierarchies [1–7]. How these hierarchies form and what makes them remain stable over time is a central question across many different fields. Social and political theorists have studied the origin of class structures and the conditions under which these structures are preserved or change [5, 8–10]. Archaeologists and other researchers from diverse fields study the factors that lead to the collapse of civilizations [11, 12]. Anthropological research has focused on the roles of norms, sanctions, and cooperative behaviour in creating and maintaining hierarchy [13, 14]. In the biological sciences, researchers have questioned whether hierarchy emerges primarily from differences in intrinsic qualities of individuals (e.g. physical strength, intelligence, or aggressive tendency) or as a self-organizing process in which a hierarchy arises as a result of many interactions between the members of the society [6, 15, 16].

From a physicist’s perspective, a fundamental question arises: Can a stable or long-lived hierarchical structure occur entirely by self-organization, based solely on inter-individual interactions, modeled as independent pair-wise “fights”? And, if so, what are the typical structures of hierarchy, and what are the characteristic times of formation and evolution of the said structures?

“Winner-loser” models are a class of mathematical models that have been used to study the self-organization of social hierarchy in biology [6, 17–22] and economics [7, 23–29]. In these models, individuals are characterized by a fitness property that determines the individual’s rank in society (such as “strength” or “wealth”). Pairs of individuals come into contact and engage in an interaction (or “fight”). The fight has a winner and a loser, and there is a rule determining the amount of fitness property transferred from the loser to the winner, and a rule determining who wins the fight. The distribution of fitness property, which changes as individuals interact with each other, represents the societal structure of the model system. While stable societal structures have been analyzed, the time evolution and intermediary, potentially long-lived societal structures have been mostly neglected.

In addition, the most obvious oversimplification of many “winner-loser” models is that any pair of individuals are equally likely to interact, regardless of their statuses. In contrast, studies of hierarchies in animal groups indicate that high status individuals spend more time and energy engaging in fights with other high status individuals than with low status individuals [30–32]. Similarly, humans are more likely to interact with members of their own social classes, especially at the extremes of the social class spectrum [33], and residential segregation, which impedes interactions between members of different social classes, is considered to be a primary factor in the creation and exacerbation of social stratification [34].

Here, we propose a new general model that addresses this oversimplification. At the same time, we focus on time evolution of the emergent societal structures. Specifically, we construct a winner-loser model in which the fitness property represents societal status. The amount of status transferred from loser to winner is proportional to the pre-fight

status of the losing individual, and we define a probability for winning that is determined by the relative statuses of the two competitors, modulated by a parameter spanning a continuous range of degree of authoritarianism from redistributive (lower-status opponent always wins) to totalitarian (higher-status opponent always wins). The latter modulation for winning has not been considered before to the best of our knowledge and it contains previous models as special cases at specific values of the authoritarianism parameter. Over a large range of parameters and excluding these special cases, we find the emergence of long-lived intermediary societal structures (distributions of societal status) for the first time. These arise independent of whether any pair of individuals are equally likely to interact or not. The latter, however, generates status distributions with more complex shapes consistent with real-world data such as household incomes. We are able to fit the simulated status distributions to USA household income data with good agreement. To our knowledge, this is the first model that produces the two-part structure of the proxy distribution by self-organization based solely on interacting individuals. The two-part structure emerges when the “original” (two-parameter) model is extended through the implementation of an additional model rule under which pairs of individuals with large differences in status fight less. We use the term “extended model” to refer to the model when this additional rule is implemented.

The original model is presented in section 2 and the extended model is presented in section 2.1. Details about the shapes of the status distributions and their evolution in time are presented in section 3. Comparison of model results to proxy data from real societies is contained in section 4. The article concludes with a summary of results and some comments regarding future research directions.

2 Definition of the model

We consider a system of N individuals, each possessing a status property, S , that determines the individual’s societal position. At each step in the simulation, a pair of individuals is randomly selected, and engages in a “fight”. The probability, p , that the higher-status individual wins the fight is expressed as a function of its status, S_1 , and that of its (lower or equal status) opponent, S_2 :

$$p = \frac{1}{1 + (S_2/S_1)^\alpha}. \quad (1)$$

When $\alpha = 1$, the probability that either individual wins is equal to the ratio of its own status to the sum of its and its opponents statuses. However, as α is tuned to values other than 1, the advantage held by the higher-status individual changes (Fig 1). As $\alpha \rightarrow \infty$, the higher-status individual is virtually guaranteed to win, regardless of how strong its opponent is. On the other hand, when α is small but positive, the higher-status individual only has a large advantage in fights against opponents with much lower status. When α is negative, $0 \leq p < 0.5$, indicating that the lower-status individual in any given fight is more likely to win. The parameter α thus generalizes previous modeling approaches, by allowing the probability for winning a pairwise fight to be continuously adjusted between end-points where the lower-status individual always wins ($\alpha = -\infty$) and where the higher-status always wins ($\alpha = \infty$).

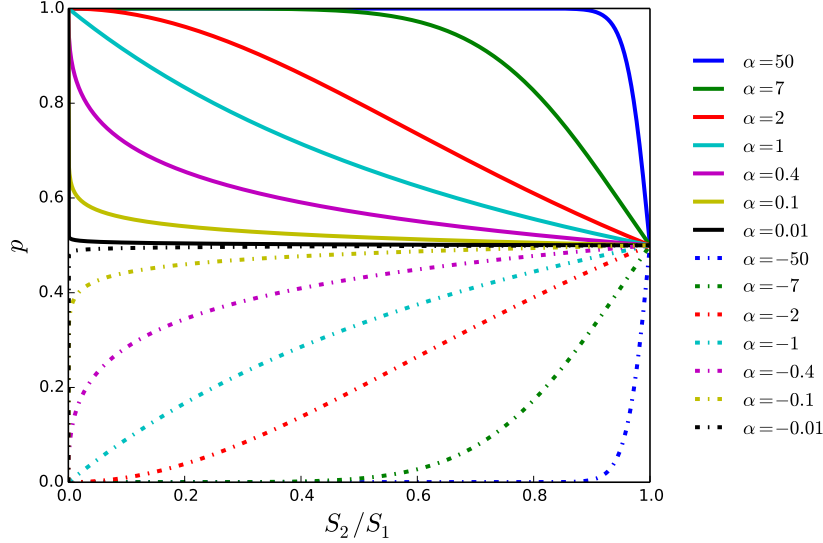


Fig 1: Probability that higher-status individual wins in a pairwise fight. The probability $p(S_2/S_1)$ (Eq 1) is shown for different values of α . Solid lines correspond to $\alpha > 0$ and dash-dotted lines to $\alpha < 0$.

To interpret the societal meaning of the parameter α , we note that the probability p depends on the relative statuses of the two individuals. This means that as long as the ratio S_2/S_1 is constant, and given a constant value of α , the probability, p , that the higher-status individual will win is constant, independent of the absolute values of S_1 and S_2 . In a general sense, the probability that a high-status individual will win in a fight against a medium-status individual is the same as the probability that a medium-status individual will win in a fight against a low-status individual. If having a higher societal status can be considered as having a higher level of “authority” in a hierarchical society, then the parameter α represents the degree to which there is deference to authority in the society or, in other words, the society’s overall level of “authoritarianism”.

Next, we explain the rule determining the amount of status transferred from loser to winner following each fight interaction. Let S_W be the before-fight status of the winner of the fight, and S_L the before-fight status of the loser. Following the fight, a portion Δ of the loser’s before-fight status is transferred to the winner, such that

$$\begin{aligned} S'_W &= S_W + \Delta \\ S'_L &= S_L - \Delta, \end{aligned}$$

where the primed quantities represent after-fight statuses. In our model, the amount of status transferred, Δ , is equal to a proportion of the before-fight status of the individual who loses the fight. That is, $\Delta = \delta S_L$, where δ is a fraction between 0 and 1. This gives us:

$$\begin{aligned} S'_W &= S_W + \delta S_L \\ S'_L &= S_L - \delta S_L. \end{aligned}$$

This rule for the amount of status transferred has realistic implications from the perspective of formation and maintenance of social hierarchy, because it means that upsets (in which the lower-status individual defeats the higher-status individual) produce large rewards for the winner and large penalties for the loser.

In an alternative rule used in many wealth distribution models [24–29], the amount of status transferred is proportional to the lesser of the two before-fight statuses. Under this “poorer scheme” rule, the reward for carrying out an upset depends only on the status of the individual who achieves the upset. Therefore, it is no better for a lower-status individual to carry out an upset against a slightly higher-status rival than against a much higher-status rival.

To illustrate the difference between these two versions of the rule, consider a society in which there are only two individuals: a high-status individual with status S_1 , and a low-status individual with status S_2 , such that $S_1 \gg S_2$. Next, imagine that the lower-status individual manages to string together a sequence of consecutive victories over the higher-status individual. In the context of dominance hierarchies, one would expect that it would take only a small number of repeated defeats of a high-status individual by the same lower-status individual before their rankings are reversed [31]. This is what occurs under the version of the rule used in our model. In the poorer scheme, however, the higher-status individual must suffer a large number of consecutive defeats before it is surmounted by the lower-status individual (for example, if $\delta = 0.25$ and $S_1 = 100S_2$, then it takes three consecutive victories under the loser scheme, and 29 consecutive victories under the poorer scheme).

Another alternative in which Δ is simply a fixed value (not proportional to the status of either competitor) is less realistic, because the amount of status transferred does not depend on the statuses of the individuals involved in the fight. For example, with this rule in place, a high status individual would gain the same amount from defeating low-status individual as from defeating high-status rival. However, some winner-loser models have made use of this rule [6, 7].

2.1 Model extension: restricting fights between individuals with large differences in status

In the “original” (two-parameter) version of our model described above, any pair of individuals are equally likely to engage in a fight, regardless of the statuses of the two selected individuals. This is an oversimplification, and evidence from studies of hierarchies in animal groups suggests that a large proportion of the status-determining interactions experienced by high status “dominant” individuals pit dominants against “challengers” who themselves have higher than average status [30–32]. Meanwhile, lower-status individuals tend not to challenge higher-status dominants, such that lower-status individuals are more likely to interact amongst themselves [30]. On the other hand, dominant individuals do interact with lower-status individuals at times, for example, through seemingly random acts of aggression which may play an important role in maintaining hierarchical rank-ordering [35].

To address the oversimplification that any pair of individuals are equally likely to interact, we implement an extension to the model via a rule that limits which individuals can fight each other based on their proximity in status. The extended model introduces two additional parameters. First, following from observations that high status individuals are more likely to engage in fights with similarly high status challengers, the new rule imposes that two selected individuals only engage in a fight if their absolute statuses are separated by not more than a threshold amount $\eta\bar{S}$. Here, $\eta \geq 0$ is a new parameter that sets the size of the threshold relative to the (conserved) average status of the system, \bar{S} , which is a natural reference point for the threshold position.

Secondly, as noted above, a realistic model should not exclude the possibility that fights between high and low status individuals will occasionally occur. Therefore, regardless of the result of the threshold criterion, the fight between the two selected individuals takes place if $r < \epsilon$, where $0 \leq \epsilon \leq 1$ is a new parameter and r is a random number such that $0 \leq r < 1$. In summation, the new rule to limit interactions based on the statuses of the two competitors can be stated as follows: two individuals are selected at random, and they fight if $S_1 - S_2 \leq \eta\bar{S}$ OR $r \leq \epsilon$. We note that, in the implementation of the simulation, this rule does not change the probability with which any two particular individuals are selected from the population, but only adds a threshold criterion to decide whether or not the fight occurs between the selected pair.

As fights take place, and status is exchanged between members of the society, a distribution of societal status takes shape. In the next section, we show the distributions of status produced by the original and extended models under different values of the parameters, and examine how these distributions evolve in time.

3 Time-evolution and structure of status distributions

In the directly following sections we focus on the original (two-parameter) version of the model first as many features are qualitatively the same as for the extended version of the model. The features specific to the extended model are then discussed in section 3.6.

3.1 Definition of time and the characteristic time τ_1

In order to discuss the shapes and time-evolution of the status distributions formed by simulations of the model, we must establish how time is defined. For simplicity and without loss of generality, we model the pairwise interactions as instantaneous such that they can be described as sequential events. We consider that one unit of time has passed once all members of the society have, on average, engaged in one pairwise interaction or fight. Under this definition of time, the rate at which an individual participates in a fight is an intrinsic frequency of the system, independent of system size, N , where N is the number of individuals in the system. Time, t , is therefore defined as $t = 2t'/N$, where t' is the number of fights that have occurred since the initiation of the simulation, and the factor of 2 comes from having each interaction involve two individuals. One unit of time is equal to $N/2$ fights.

Previous work by Ispolatov et al. [23] shows the existence of a characteristic time in a model that is mathematically equivalent to our original (two-parameter) model in the case where $\alpha = 0$. An analytic solution for the time evolution of the variance of the status distribution (wealth distribution, in Ref. [23]) was found to be as follows:

$$M_2(t) = \frac{\delta \bar{S}}{1 - \delta} \left(1 - e^{-\delta(1-\delta)t} \right), \quad (2)$$

where the variance (second central moment) $M_2(t)$ can be calculated directly from the status distribution:

$$M_2(t) = \sigma^2(t) = \frac{\sum_{i=1}^N (S_i(t) - \bar{S})^2}{N}, \quad (3)$$

where $S_i(t)$ is the status of individual i at time t , and \bar{S} is the (conserved) average status.

Similar to Eq 2, higher moments of the status distribution converge to constant values, and the status distribution attains a steady state. Eq 2 therefore shows that the variance approaches a steady-state value of $M_2 = \delta \bar{S} / (1 - \delta)$ at large times and that the approach to the steady-state is characterized by a time constant equal to $(\delta(1 - \delta))^{-1}$. Eq 2 can be re-written in a form that is useful for our purposes:

$$M_2 = c_1(1 - e^{-t/\tau_1}), \quad (4)$$

where c_1 and τ_1 are generally functions of δ and α . In the following, we use the symbols \hat{c}_1 and $\hat{\tau}_1$ to represent these functions when $\alpha = 0$, such that $\hat{\tau}_1 = (\delta(1 - \delta))^{-1}$ and $\hat{c}_1 = \delta \bar{S} / (1 - \delta)$, as per Eq 2. Appendix S1.A contains a demonstration that our definition of time corresponds to how time is defined in the analytical result in Eq 2.

3.2 Overview of status distributions produced by the model

In order to explore the societal structures generated by the model, we begin by setting $\alpha = 0$. In this limiting case, $p = 0.5$ for all fights, regardless of the statuses of the competitors (see Eq 1) and, importantly, there always results a stable steady-state status distribution. As was noted in section 3.1, when $\alpha = 0$, our model is mathematically equivalent to the model of Ispolatov et al. [23]. Those authors found an analytical solution for the functional form of the distribution when $\delta = 0.5$ and showed that the tail of the distribution decays exponentially for all values of δ . We show graphs of distributions for several values of δ when $\alpha = 0$ and their evolutions from initial condition to steady-state, as a basis for comparison with model results for which $\alpha \neq 0$, presented further below.

Fig 2 shows the time evolution of systems prepared in an “egalitarian” initial condition, in which all individuals have the same initial status of $S = 1$. Each row in the figure corresponds to a different value of δ , and each column to an instant in time, with time increasing from left to right across the subplots. For all values of δ , the system undergoes an early-time evolution away from the initial condition. Once the system has passed through the initial transient period, it arrives at a steady-state in which the distribution remains constant in time. The steady-state distribution is obtained within a time equal

to a few multiples of $\hat{\tau}_1$, as expected from Eq 4. The shape of the steady-state distribution varies from more egalitarian (small standard deviation) for smaller δ to more unequal (large standard deviation) for larger δ .

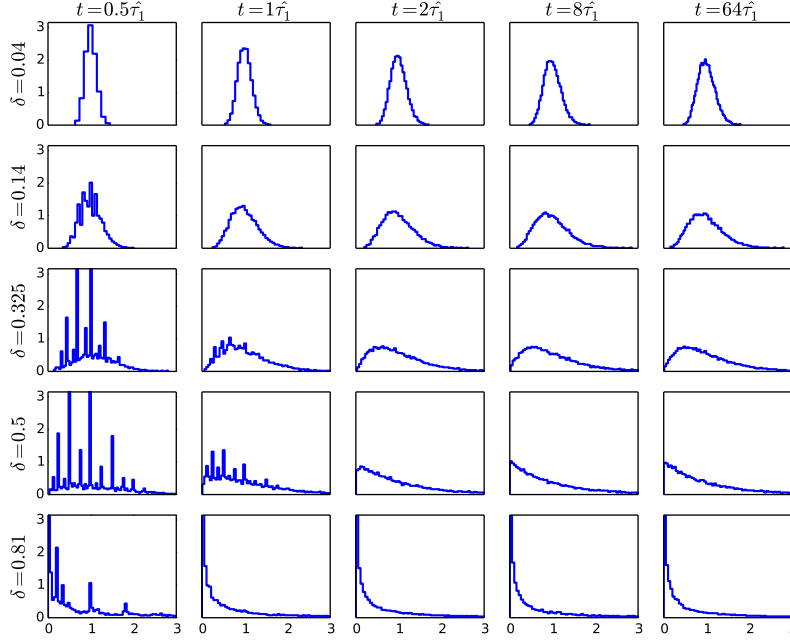


Fig 2: Evolution of status distribution from initial condition to steady-state. Time evolution of status distributions when $\alpha = 0$, for different values of δ , starting from an egalitarian initial condition. Each column corresponds to a different instant in time and each row to a value of δ . x-axes correspond to status, S , and y-axes to the probability density, $p(S)$. Results are for system size $N = 1000$, and $n_r = 20$ realizations of the simulation.

The steady-state distributions from Fig 2 are plotted together in Fig 3, along with the time evolution of the standard deviation, σ (inset). As expected from Eq 2, σ approaches a steady-state plateau with a value of $\hat{c}_1^{1/2}$. The skewness μ_3/σ^3 , where μ_3 is the third central moment of the distribution, also arrives at a steady-state plateau at large time (grey lines in inset of Fig 3). The plateau in μ_3/σ^3 is equal to two times that of the plateau in σ , as can be shown by solving for the third moment following the approach presented in Ref. [23].

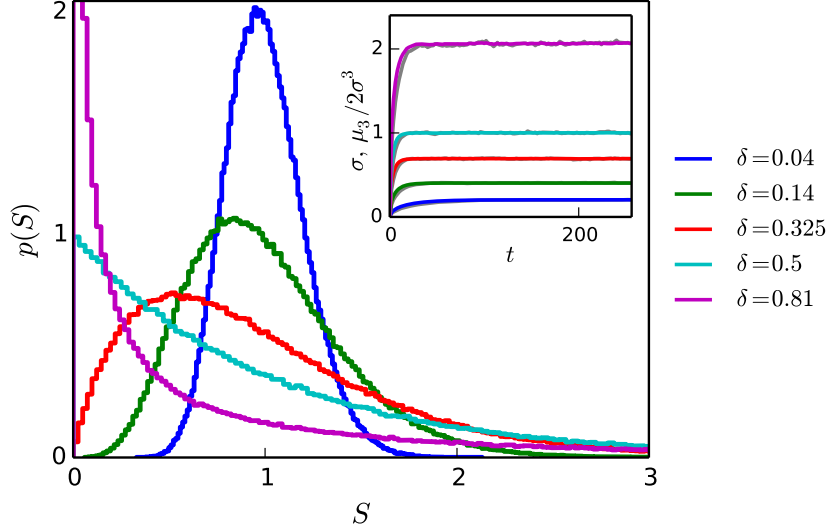


Fig 3: Shape of steady-state status distribution as a function of δ . Steady-state status distributions for various values of δ , with $\alpha = 0$. Inset: plateau in σ (coloured) and skewness (grey) indicate that status distributions are in steady-state. Values of δ indicated in figure legend. Distributions obtained after simulating up to time $t = 64\hat{\tau}_1$. $N = 10^5$, $n_r = 5$.

Next, we look at the time evolution of distributions of societal status when the value of the authoritarianism $\alpha > 0$. Fig 4 shows distributions for the same values of δ shown in Fig 2, but now with $\alpha = 0.2$ (green) and $\alpha = 0.5$ (blue). For both values of α , after a time $t = \hat{\tau}_1$ has elapsed, the model produces status distributions with similar shapes to the steady-state distributions shown in Fig 2, for the corresponding values of δ . However, as time increases, the shape of the status distribution continues to change. For example, when $\delta = 0.81$, after a time $t = 64\hat{\tau}_1$ has elapsed, the distributions for both $\alpha = 0.2$ and $\alpha = 0.5$ are highly skewed, such that virtually all individuals have near zero status, and a small minority have very large statuses (larger than the scale of the subplot).

For smaller values of δ , the evolution of the status distribution away from its shape at $t = \hat{\tau}_1$ occurs more slowly, such that the status distribution appears to remain virtually unchanged over the observation period (e.g. from $t = 8\hat{\tau}_1$ to $t = 64\hat{\tau}_1$ for $\delta = 0.04$ and $\delta = 0.14$ when $\alpha = 0.2$, and from $t = 8\hat{\tau}_1$ to $t = 64\hat{\tau}_1$ for $\delta = 0.04$ when $\alpha = 0.5$). A different initial condition, in which the initial status of each individual is chosen randomly from a uniform distribution with average status $\bar{S} = 1$ produces qualitatively the same results regarding the time evolution of the status distributions (Appendix S1.B).

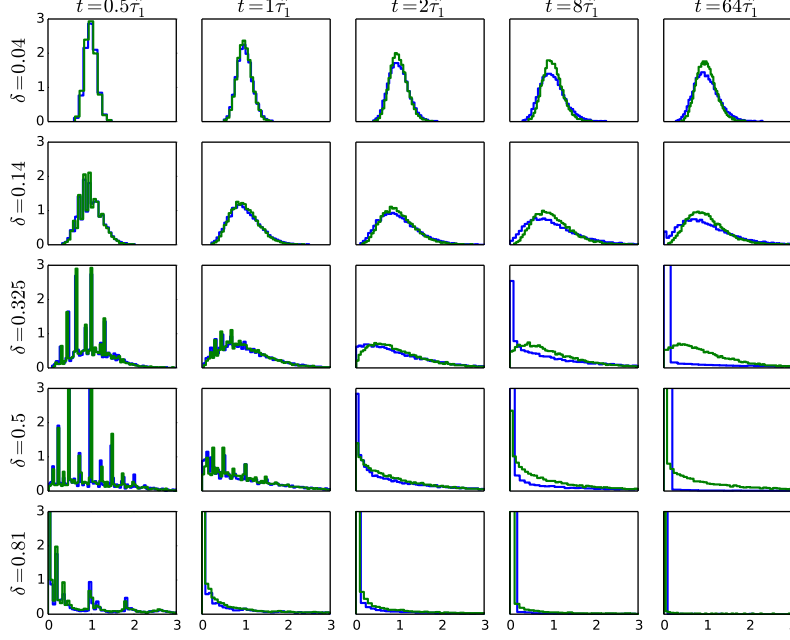


Fig 4: Evolution of status distributions when $\alpha > 0$. Time evolution of status distributions for different values of δ , with $\alpha = 0.2$ (green) and $\alpha = 0.5$ (blue), starting from an egalitarian initial condition. Each column corresponds to a different instant in time and each row to a value of δ . x-axes correspond to status, S , and y-axes to the probability density, $p(S)$. $N = 10^3$, $n_r = 20$.

Fig 5 provides a closer look at how the shapes of the potentially transient distributions of status at a fixed time change as α is increased, with δ fixed equal to 0.14. The curve for $\alpha = 0$, $\delta = 0.14$ from Fig 3 is reproduced in Fig 5, along with the inset, showing that $\sigma(t)$ undergoes an initial transient period before arriving at a plateau value for times $t \gg \hat{\tau}_1$.

For large values of $\alpha > 0$ ($\alpha = 0.6$ and $\alpha = 0.8$), the inset of Fig 5 shows a rapid increase of $\sigma(t)$ that continues beyond the initial transient period. The status distributions are rapidly evolving (“running away”) toward a totalitarian end-state in which a single individual possesses virtually all of the societal status of the system and all other individuals have status approaching zero (Appendix S1.F contains a proof that only one individual with non-negligible status remains in the totalitarian end-state).

For smaller values of $\alpha > 0$ ($\alpha = 0.2$ and $\alpha = 0.4$), $\sigma(t)$ appears to be virtually unchanged in the time period following the initial transient period shown in Fig 5. Yet,

as we show below (sections 3.3 and 3.4), $\sigma(t)$ does increase with t , albeit much more slowly, such that the status distributions can be considered to be in a long-lived state.

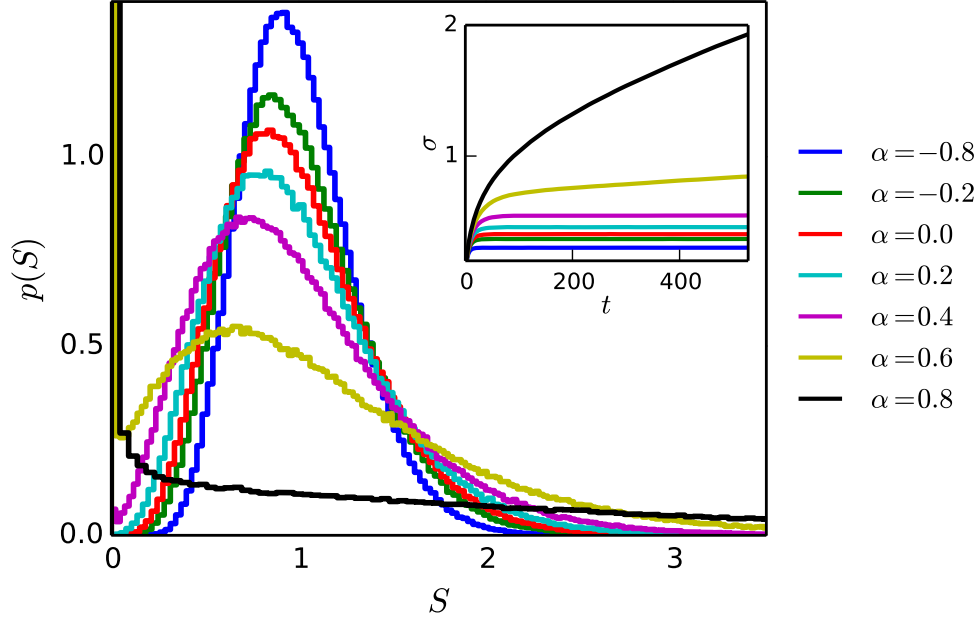


Fig 5: Shape of status distribution as a function of α . Status distributions for various values of α in the range $[-0.8, 0.8]$, with $\delta = 0.14$. Distributions obtained after simulating up to time $t = 64\hat{\tau}_1$. $N = 10^5$, $n_r = 5$.

Fig 5 also shows the status distributions that arise when $\alpha < 0$. For this region of parameter-space, the lower-status individual has a higher probability of winning the fight than the higher-status individual. Our numerical simulations show that the distributions are in steady-state (as for $\alpha = 0$) and become more egalitarian (smaller σ) as α is decreased while δ is held constant.

3.3 Long-lived behaviour

In this section we quantify the time evolution and the long-lived behavior of the status distributions produced by the model by examining the evolution of $M_2(t)$ for $\alpha > 0$ (plots in Fig 6a-c). As noted in section 3.2 and demonstrated in Appendix S1.F, for large values of α , the status distribution runs away to an end-state in which a single individual possesses virtually all of the society's status, and all other individuals have virtually zero status. In this totalitarian end-state, the variance M_2 approaches an upper plateau

$$c_2 = (N - 1)\bar{S}^2 = N - 1, \quad (5)$$

where the average status is defined in the model to be $\bar{S} = 1$, without loss of generality. The upper plateau c_2 is the maximum possible value of M_2 . For finite-sized systems, M_2

risers to this upper plateau at large times. This large-time ascent to c_2 happens quickly for large values of α , and much more slowly for smaller values of α (main plot of Fig 6a).

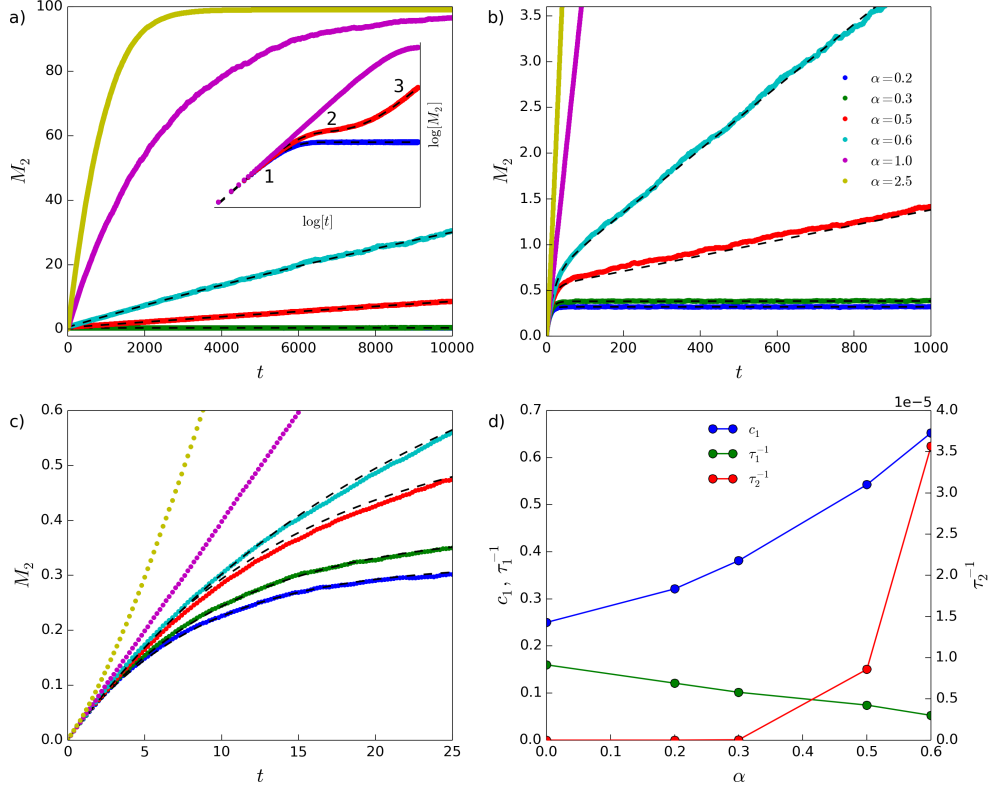


Fig 6: Evolution of $M_2(t)$ for $\alpha > 0$. Values of α are indicated in the legend in (b), and $\delta = 0.2$ for all curves. (a) shows rapid ascent of $M_2(t)$ to upper plateau value for $\alpha = 1.0$ and $\alpha = 2.5$ (main plot), and the inset of (a) shows three of the curves on log-log scale, with stages 1-3 of the evolution of $M_2(t)$ indicated for the $\alpha = 0.5$ curve. (b) and (c) show the main plot of (a) at different magnifications, to allow inspection of the fit of Eq 6 (dashed black lines) to the curves with $\alpha \leq 0.6$. (d) fit parameters, with y axis scale for τ_2^{-1} shown on righthand side (parameters for $\alpha = 0$ are from Eq 6, assuming $\tau_2 = \infty$). $N = 100$, $n_r = 500$.

There therefore appear to be two relevant time-scales in the dynamics of the status distributions: one controlling the evolution away from the initial condition, and a second controlling the long-time approach to the totalitarian end-state. To capture the dynamics of $M_2(t)$ for $\alpha > 0$, we attempt to fit, to the simulation data, a sum of exponential functions:

$$M_2 = c_1(1 - e^{-t/\tau_1}) + (c_2 - c_1)(1 - e^{-t/\tau_2}), \quad (6)$$

where τ_2 is a characteristic time controlling the rate of approach of M_2 to the upper plateau. The first term in Eq 6 relates to the short-time dynamics of the status distribution, while the second term relates to the long-time dynamics. Long-lived states are

produced for values of the model parameters α and δ for which τ_2 is much larger than the time, τ_{obs} , over which the system is observed (simulated), and τ_1 . When $\tau_1 \ll t \ll \tau_2$, Eq. 6 becomes $M_2(t) \approx c_1(1 - e^{-t/\tau_1})$ where, for $\alpha > 0$, c_1 represents an operational plateau value of $M_2(t)$ corresponding to the long-lived state.

Fits of Eq 6 to simulated data are shown by the black dashed lines in Fig 6, for the four smaller values of α . For these fits, c_2 is fixed at its upper plateau value $c_2 = N - 1$. Although the fits are imperfect (Fig 6c), they do appear to capture the short-time “elbow” controlled by τ_1 and c_1 , and the long-time ascent toward the upper plateau controlled by τ_2 (Fig 6b). Fig 6d shows the fit parameters as functions of α : as α is increased, both c_1 and τ_1 increase, resulting in a slower evolution of M_2 (and therefore, of the shape of the status distribution) away from the initial condition. On the other hand, as α increases, τ_2 decreases, leading to a more rapid (long-time) approach to the upper plateau. As α is increased to larger values, it becomes difficult to resolve the early-time “elbow”, and thus difficult to obtain a meaningful fit of Eq 6. Furthermore, as shown in Fig 6c, the shape of $M_2(t)$ appears to approach a straight line (at early times) as $\alpha \rightarrow 1$, and then, to bend upwards away from such an initial straight line when $\alpha > 1$.

For small $\alpha > 0$, the status distributions pass through three phenomenological stages, beginning with an egalitarian initial condition and ending in the totalitarian end-state (see Appendix S1.E for details). In particular, the first stage pertains to the evolution of the status distribution away from its initial condition over time scales of the order τ_1 and into a distribution with a form similar to that of the $\alpha = 0$ steady-state distribution. This “stage 2” distribution changes only very slowly, eventually transitioning into a stage (“stage 3”) where high status individuals are nearly guaranteed to win all fights. The duration of stage 2 decreases and essentially disappears as α is increased, explaining the inability of Eq 6 to represent $M_2(t)$ for larger values of α . In the asymptotic state of the evolution $t \gg \tau_2$, all individuals have $S \approx 0$, except for a single dominant individual with status equal to the total status of the system.

Our findings are largely independent of the system size N . As shown explicitly in the SI (Appendix S1.C), the parameters controlling the early-time behaviour of M_2 (c_1 and τ_1) remain constant as the system size, N , is increased, whereas the parameters controlling the long-time behaviour of M_2 (c_2 and τ_2) both scale linearly with N . A proof that the time required to reach the end-state, τ_{end} , scales linearly with N in the extreme scenario where $\delta = 1$ and $\alpha = \infty$ is also included in Appendix S1.D, as a demonstration of the configurational reasons why the long-time (approach to the end-state) evolution of the model dynamics increases in proportion to the system size N .

3.4 Phenomenology of the characteristic time τ_2 when $\alpha > 0$

The characteristic time τ_2 increases as α is decreased from large positive values, as shown in Fig 6d. We also know, from comparison of Eqs 2 and 6, that $\tau_2 = \infty$ when $\alpha = 0$. In order to further explore the relationship between τ_2 and α , we consider an analogy with barrier-like or “activated” processes typical of many physical systems [36]. We find that the resulting Arrhenius equation provides a good description of the relationship between τ_2 and the model parameters α and δ .

The rate of an activated process is proportional to an exponential term containing an energy barrier scaled by temperature. The exponential term is multiplied by a pre-factor called the attempt frequency, which is typically independent of temperature. This type of relationship between rate and temperature can be found in many diverse physical phenomena, including the rate of chemical reactions [36], the relationship between diffusion coefficients and temperature [36], the rate of nucleation according to the classical nucleation theory [37], the viscosity of strong glass-formers [38], and the blocking transition in superparamagnetism [39], as well as in biology regarding, for example, the rate of chirping in crickets and of flashing in fireflies, and in psychology, where human perception of time is related to body temperature through a relationship of this form [40].

If the characteristic time τ_2 is regulated by α according to an activated process, then one would expect the relationship between τ_2 and α to follow an Arrhenius equation of the form:

$$\frac{1}{\tau_2} = f_0 e^{-\alpha_b/\alpha}, \quad (7)$$

where α_b is a term that plays a role similar to an energy barrier in an activated process and f_0 is analogous to an attempt frequency. To test this idea, we plot the logarithm of N/τ_2 vs. α^{-1} in Fig 7. The factor of N is included due to the fact that τ_2 scales linearly with N , as discussed in section 3.3 and shown in Appendix S1.C.

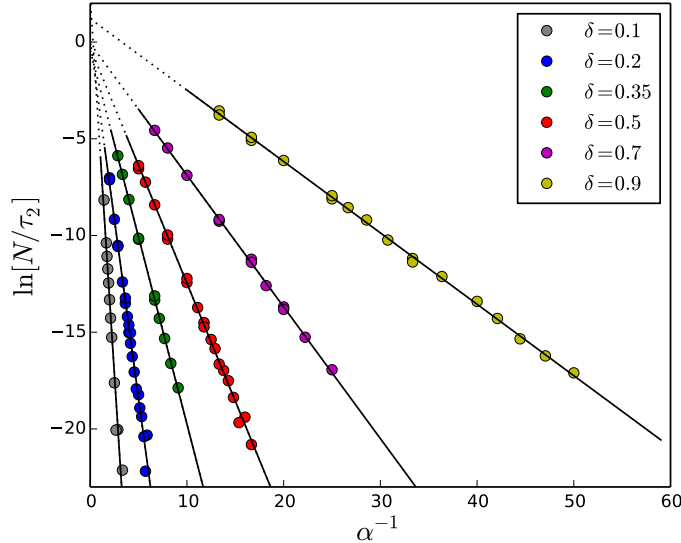


Fig 7: Arrhenius relationship between τ_2 and α . Plots of $\ln[N/\tau_2]$ vs. α^{-1} for various values of δ confirm the relationship proposed in Eq 7. The slope of each linear fit is $-\alpha_b(\delta)$. A discussion regarding the evaluation of errors on the extracted values of τ_2 is included in Appendix S1.G.

The linear behaviour seen in Fig 7 confirms the relationship between τ_2 and α proposed in Eq 7. In the figure, the δ -dependent slopes of the linear fits correspond to $-\alpha_b$, and the intercepts to $\ln[Nf_0]$. The values of α_b extracted from the linear fits in Fig 7 are shown as a function of δ in Fig 8. As can be seen, α_b diverges as δ is decreased. The red line in Fig 8 shows the function $\alpha_b = 0.53\delta^{-1.21}$.

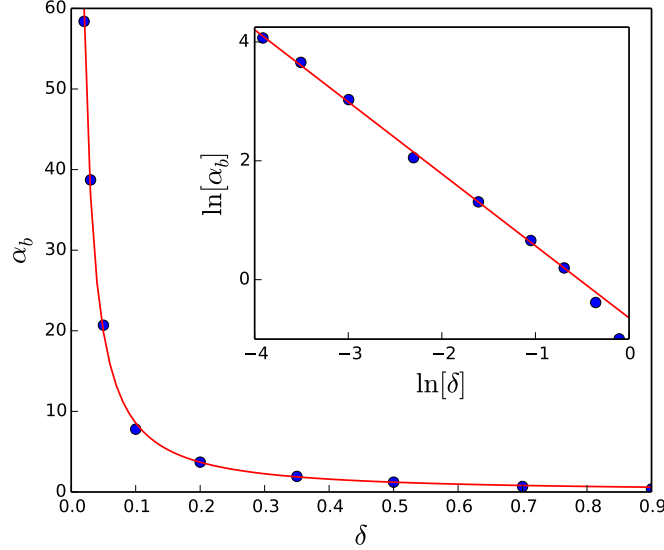


Fig 8: Divergence of α_b with decreasing δ . The red line in the main plot and inset corresponds to $\alpha_b = 0.53\delta^{-1.21}$.

In Fig 7, the y-intercepts of the linear fits appear to cluster around 0, suggesting that the prefactor Nf_0 in the expression for N/τ_2 following from Eq 7 is of the order of 1 for the values of δ considered. The y-intercepts do not, however, give a robust determination of the prefactor Nf_0 . This may be due to a change in functional form of Eq 6 as α increases such that τ_1 vanishes. Alternatively, the prefactor Nf_0 can be directly determined by setting $\alpha = \infty$ (equivalent to $p = 1$ in Eq 1) in the simulations and extracting $\tau_2(\alpha = \infty)$ from $M_2(t)$. In so doing, we have assumed that $t \gg \tau_1$ and $c_2 \gg c_1$ such that Eq 6 becomes $M_2(t) \approx c_2(1 - e^{-t/\tau_2})$. Nf_0 is then equal to $N/\tau_2(\alpha = \infty)$. This approach provides more robust determinations of Nf_0 , which are shown in Fig 9, along with a fit (red line) of the function $Nf_0 = 1.03\delta^{1.28}$.

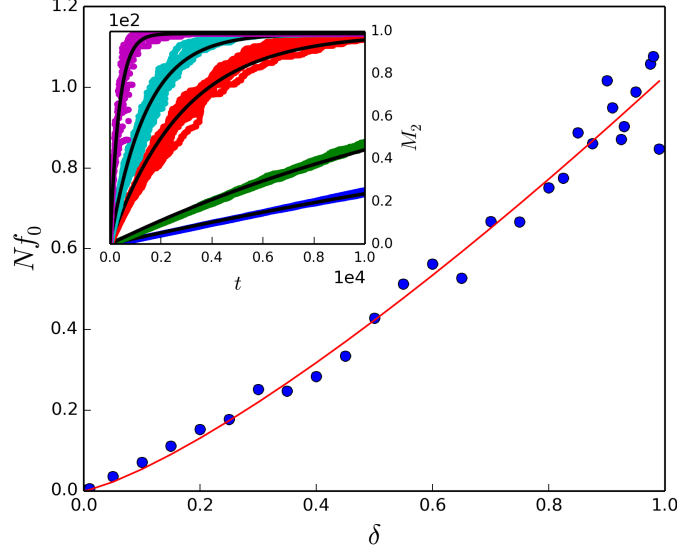


Fig 9: Nf_0 as a function of δ . The red line in the main plot corresponds to $Nf_0 = 1.03\delta^{1.28}$. Simulation data generated for system size $N = 100$. Inset: selected plots of $M_2(t)$ where $\alpha = \infty$, and $n_r = 10$ realizations are shown overlaid on top of each other, for values of δ as follows: 0.005 (blue), 0.01 (green), 0.05 (red), 0.1 (cyan), 0.4 (magenta); black line shows fit of $M_2(t) \approx c_2(1 - e^{-t/\tau_2})$, from which $\tau_2(\alpha = \infty)$ is extracted.

Substituting the expressions for Nf_0 and α_b into Eq 7 gives:

$$\frac{N}{\tau_2} \approx 1.03\delta^{1.28}e^{-0.53/(\alpha\delta^{1.21})}. \quad (8)$$

Eqs 7 and 8 show that τ_2 diverges exponentially as $\alpha \rightarrow 0$. This is consistent with Eq 2, which indicates that $\tau_2 = \infty$ when $\alpha = 0$. Moreover, the parameter δ appears in both the pre-factor and the argument of the exponential of Eq 8, such that as $\delta \rightarrow 0$, $\tau_2 \rightarrow \infty$, regardless of the value of α . This is consistent with the fact that for $\delta = 0$ no status is exchanged during a pairwise interaction and the initial status distribution is trivially stable. These observations strongly suggest that stable status distributions only exist for $\alpha \leq 0$ as well as $\delta = 0$. When $\alpha > 0$, Eq 8 allows us to identify the time scale of the transition between long-lived societal structures and runaway toward the totalitarian end-state as we discuss in more detail below.

3.5 $\delta - \alpha$ phase diagram and equi-sigma distributions

As shown in sections 3.2-3.4, for all positive values of δ , the model gives rise to three regions of behaviour: true steady-state status distributions ($\alpha \leq 0$), long-lived status distributions that eventually arrive at the totalitarian end-state (small values of $\alpha > 0$), and runaway (rapid evolution) toward the totalitarian end-state (large values of $\alpha > 0$). The transition between true steady-state and long-lived behaviour occurs due to an

exponential divergence of the characteristic time τ_2 as $\alpha \rightarrow 0^+$. Runaway behaviour occurs when a noticeable slope is observed in the evolution of $\sigma(t)$ (see the inset of Fig 5 for $\alpha = 0.6$ and $\alpha = 0.8$). Whether such a slope is observed or not depends on $\tau_2(\delta, \alpha)$ and on the time, τ_{obs} , over which the system is observed. The location, in $\delta - \alpha$ parameter-space, of the transition between long-lived and runaway behaviours therefore depends on τ_{obs} , and can be determined directly from the data or via Eq 8, as described below. The three regions and the transitions between them can be summarized in a $\delta - \alpha$ phase diagram as shown in Fig 10.

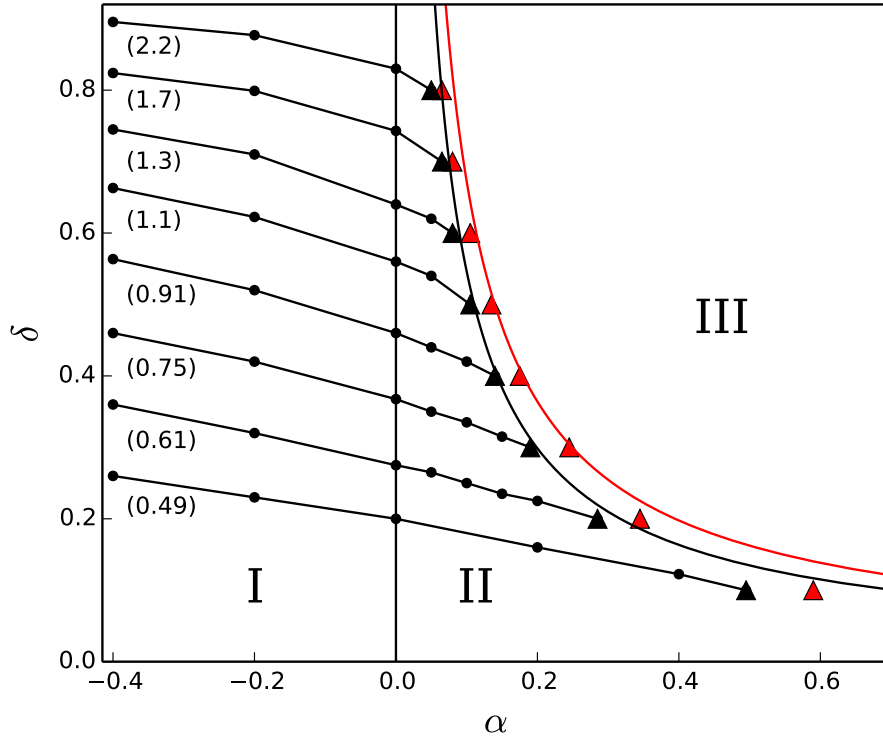


Fig 10: $\delta - \alpha$ phase diagram. The model exhibits three regions of behaviour in $\delta - \alpha$ parameter-space: I ($\alpha \leq 0$ or $\delta = 0$): true (infinite-duration) steady-state status distributions; II (small values of $\alpha > 0$): long-lived status distributions; III (large values of $\alpha > 0$): runaway behaviour. Within regions I and II, equi- σ lines (lines of equal standard deviation of the status distribution) are shown with σ values indicated in parantheses below each equi- σ line. The location of the transition between regions II and III is observation time-dependent, and is marked by the black triangular points for $\tau_{obs} = 10^4$ and by the red triangular points for $\tau_{obs} = 10^3$, as determined directly from the simulation data. The location of the transition as determined by the Arrhenius relation between τ_2 and α is shown by the black ($\tau_{obs} = 10^4$) and red ($\tau_{obs} = 10^3$) curves. System size $N = 1000$.

While α largely determines the stability of the asymptotic status distributions, the exact value of $\delta > 0$ influences the shape of the status distribution, as already seen for $\alpha = 0$ in section 3.2. This is also true for the long-lived distributions. Essentially identical distributions can be produced (within a particular simulation time) for different combinations of the parameters δ and α : Fig 11 shows status distributions generated for three different points in δ – α parameter-space. The inset to Fig 11 shows the distributions with a logarithmic scale on the y-axis, in order to allow closer inspection of the tails of the distributions. To compare the shapes of the distributions in Fig 11, in addition to visual inspection of the plotted curves, we use the time-and-realization-averaged standard deviation, $\langle\sigma\rangle$ of the status distributions. This is defined as follows: first, we average the standard deviation of the status distributions over 500 realizations of the simulation, giving us $\sigma(t)$. Then, we average $\sigma(t)$ over a range of time ($500 \leq t \leq 1000$) during which $\sigma(t)$ is approximately constant corresponding to the long-lived state. This gives us $\langle\sigma\rangle$. Repeating this procedure for the skewness of the status distributions gives us $\langle\mu_3/\sigma^3\rangle$, which we also use to compare the shapes of the distributions in Fig 11.

The value of $\langle\sigma\rangle$ for the three distributions is the same, within error (caption of Fig 11). The error value used here is the standard deviation of $\sigma(t)$ taken over the range of time $500 \leq t \leq 1000$. Likewise, $\langle\mu_3/\sigma^3\rangle$ is the same, within error, for the three different distributions. There is, however, one subtle difference between the distributions that can be seen in Fig 11: the value of $p(S)$ at $S = 0$ becomes systematically larger going from smaller (larger) to larger (smaller) α (δ). Except for this caveat, Fig 11 shows the existence of sets of (δ, α) points producing essentially identical distributions. Sets of such points, for different values of $\langle\sigma\rangle$, are plotted as “equi- σ ” lines in Fig 10.

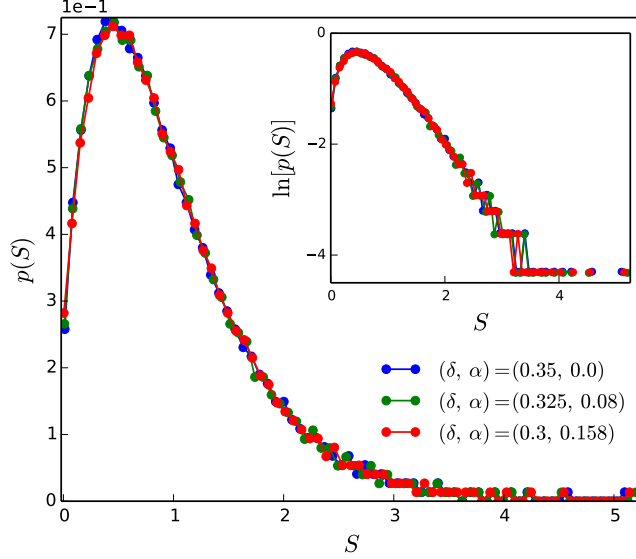


Fig 11: Equi- σ status distributions. Status distributions obtained at $\tau_{obs} = 1000$, for different pairs of (δ, α) values. Blue curve: $\langle \sigma \rangle = 0.733 \pm 0.001$; green curve: $\langle \sigma \rangle = 0.732 \pm 0.001$; red curve: $\langle \sigma \rangle = 0.732 \pm 0.001$. $\langle \mu_3 / \sigma^3 \rangle = 1.46 \pm 0.01$ for all three distributions.

The location of the transition between regions II and III of Fig 10 depends on the time, τ_{obs} , over which the system is observed (simulated). We determined the location of this transition in two ways. First, we used a simple criterion to equate the onset of runaway with the appearance of a positive slope in the long-time portion of $M_2(t)$. In this way, the long-lived state corresponds to a plateau value of $M_2(t)$ over a particular τ_{obs} (where $\tau_{obs} \gg \tau_1$). The long-lived state is considered to be lost when, instead of a plateau, a positive slope is observed in $M_2(t)$ after a time τ_{obs} has transpired. The black and red triangular markers in Fig 10 indicate the onset of runaway as determined by this criterion, for $\tau_{obs} = 10,000$ and $\tau_{obs} = 1,000$, respectively. Secondly, the location of the transition can be determined using the Arrhenius relation presented in section 3.4 to determine the value of α for which $M_2(t)$ increases by a sufficient amount after a time τ_{obs} has transpired. The location of the transition as determined by the Arrhenius relation is shown by the curving black and red lines in Fig 10. Details about how these two approaches were conducted are contained in Appendix S1.H.

3.6 Status distributions in the extended model

In section 2.1, we presented a simple extension to the original (two-parameter) model that restricts which individuals can fight each other based on the proximity in their statuses. This “extended model” introduces two new parameters: η , which sets a threshold $\eta \bar{S}$ (where \bar{S} is the average status of the system), such that individuals with statuses separated by an amount more than this threshold are restricted from fighting with each

other; and ϵ , the probability with which two individuals that have a separation of statuses greater than $\eta\bar{S}$ do nevertheless fight each other.

Fig 12 shows distributions of status generated by simulations of the extended model. A log-linear scale is used in the righthand column of plots to allow inspection of the high-status tails of the status distributions. In all subplots, $\alpha = 0$ and $\delta = 0.2$. When $\epsilon = 1$ (Fig 12a-b) the original (two-parameter) model is recovered, such that the parameter η has no effect on the shape of the status distribution. Also, when $\epsilon = 1$, the high-status tail of the distribution decays exponentially, in accordance with the analytic result found by Ispolatov et al. [23] (Fig 12b). As ϵ is decreased, a “break” in the high-status tail of the distribution emerges, as can be seen in the log-linear plots in Fig 12d, f, and h. Following this break, the distribution enters a second exponentially-decaying regime (black dashed line in Fig 12f) that ends with a cutoff. Increases to η cause the location of the break as well as the location of the peak of the distribution to shift to higher values of S . The plateaus in $\sigma(t)$ (insets in Fig 12) for $\epsilon > 0$ indicates that these distributions are in steady-state.

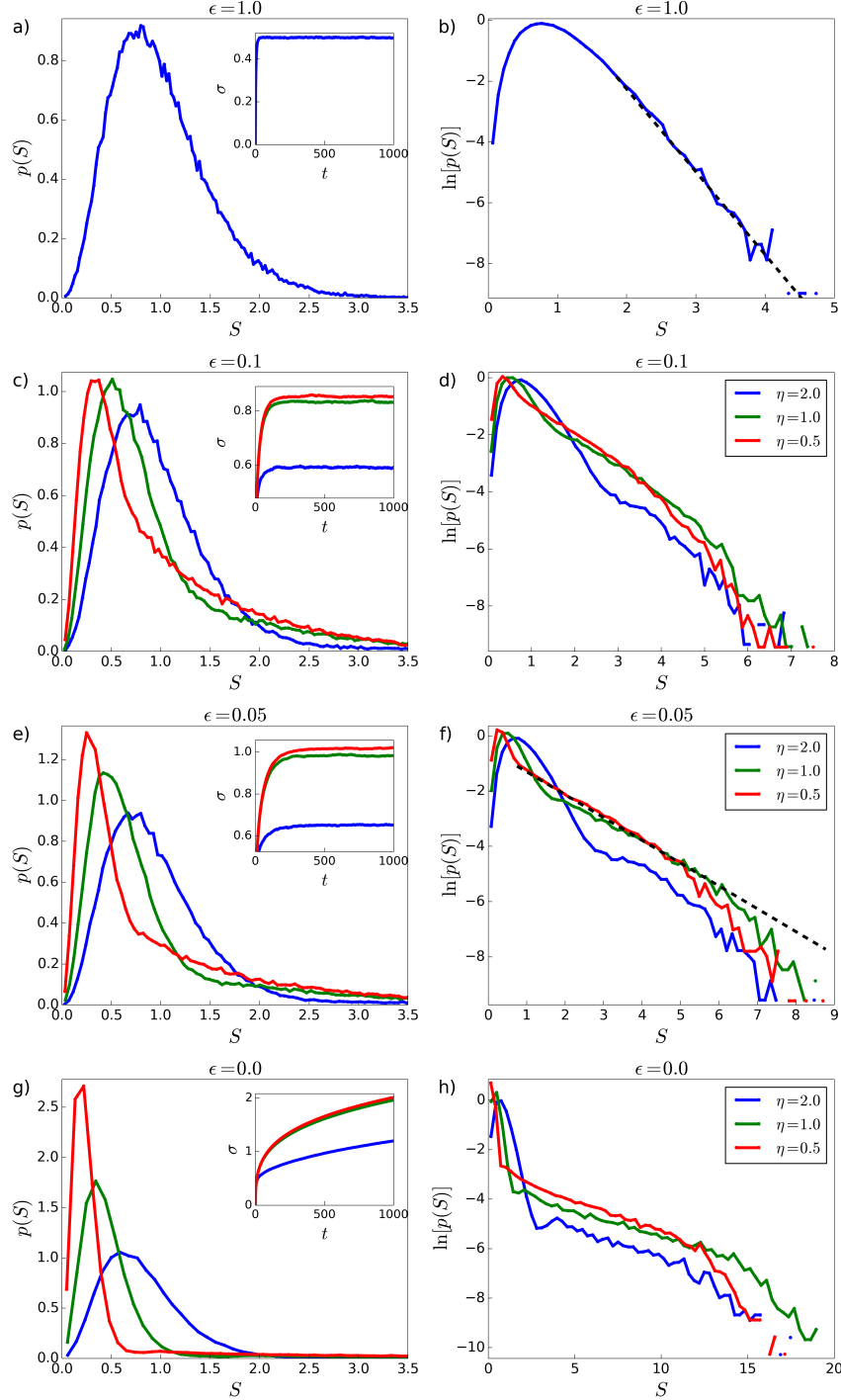


Fig 12: Status distributions in the extended model. $\delta = 0.2$ and $\alpha = 0$ in all plots. Plots b, d, f, and h show the distributions on a logarithmic scale, in order to allow for inspection of the large- S tail. The black dashed lines in (b) and (f) are maximum likelihood fits of exponential distributions with lower-bound at $S = 2.25$ in (b) and [lower-bound, upper-bound] at $S = [0.75, 5.0]$ in (f), where plotted fit line in (f) is extrapolated beyond $S = 5.0$. System size $N = 10^5$.

When $\epsilon = 0$ (Fig 12g and h), $\sigma(t)$ does not obtain a plateau and continues to increase over the duration of the simulation time. These distributions are approaching an end-state in which the majority of individuals have status approaching zero, and a small minority of individuals have large statuses. In this end-state, the few high-status individuals are prevented from interacting with each other because their statuses are separated by amounts greater than $\eta\bar{S}$. The specific configuration of the $\epsilon = 0$ end-state depends on the particular sequence of interactions. A positive value of ϵ is therefore needed in order for the simulation to obtain a steady-state.

In all of the plots in Fig 12, $\alpha = 0$. The distributions produced with $\alpha = 0$, $\eta > 0$, and $\epsilon > 0$ show a plateau in $M_2(t)$. When $\alpha > 0$, $M_2(t)$ behaves qualitatively in the same way as the original (two-parameter) model. That is, a long-lived state is observed for small values of $\alpha > 0$, and a runaway for large values of $\alpha > 0$, where the location of the transition between the long-lived state and runaway depends on the observation (simulation) time. Several figures showing how the extended model distributions evolve for representative values of $\alpha > 0$ are included in Appendix S1 (part I).

4 Comparison of model distributions with real-world data

Our model is based on the simple premise that each individual in a society is characterized by a single quantity, the individual's status, S . A person's real-world societal status is a complex quantity that is difficult to define and measure. For example, researchers have attempted to define socioeconomic status as a combined measure of income, education, occupation, and wealth [41]. For the purpose of tentative comparisons with real-world data, and not having defined S beyond its operational meaning within our model, we use household income in Canada and the USA as a proxy for societal status in those countries. Advantages of using income data as a proxy include that it is readily available in online datasets for these two countries and that it is quantitative, making it straightforward to analyze and compare to our model results. We use household income, rather than personal income, as our proxy for societal status, in order to avoid artifacts related to income sharing within a nuclear family unit, such as when a spouse decides not to work or to work below his or her maximum market value.

4.1 Canadian income distribution

Fig 13 shows the (pre-tax) distribution of Canadian household incomes from the 2001 Canadian census [42], as well as a model-generated status distribution for the two-parameter version of our model (section 2). The simulated system contained $N = 312,513$ individuals, which is the number of households in the public-use census sample. The average status of each individual was set equal to the average household income in the data, such that $\bar{S} = 55,536$. The model parameter α was set equal to 0, in order to produce true steady-state status distributions. The parameter δ was then adjusted until a good fit was obtained with the income data ($\delta = 0.35$ for the plot in Fig 13).

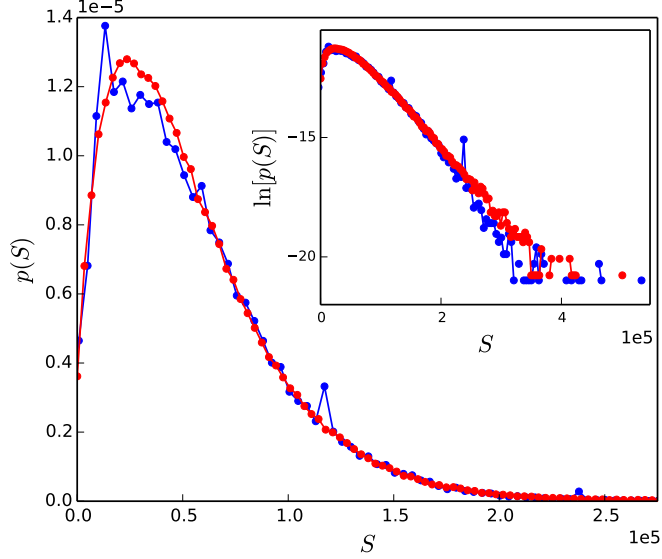


Fig 13: Fit of original (two-parameter) model status distribution to Canadian household income distribution. Simulated distribution (red curve, $\delta = 0.35$ and $\alpha = 0$), compared to the distribution of Canadian household incomes from the year 2000 (blue curve). Scaled standard deviation, $\sigma/\mu = 0.732$ and skewness, $\mu_3/\sigma^2 = 1.3$ for the simulated distribution, and $\sigma/\mu = 0.731$ and $\mu_3/\sigma^2 = 1.4$ for the proxy distribution. The x-axis of the main plot has been cut at $S = 2.5 \times 10^5$. The large peak in the data at \$12,000 ($S = 0.12 \times 10^5$) is most likely due to welfare benefits provided by the government, and the peak at \$120,000 ($S = 1.2 \times 10^5$) comes from an upper income cutoff applied to the public-use data by Statistics Canada [44].

Although α was set equal to 0 in Fig 13, in section 3.5 we showed that essentially the same long-lived status distributions can be obtained for (δ, α) values that trace out an equi- σ line in $\delta - \alpha$ parameter-space (see Fig 10). Starting with a given value of δ and $\alpha = 0$, one can locate an equi- σ line in Fig 10. Then, following the equi- σ line in the direction of increasing α , one eventually arrives at the transition between long-lived states and runaway (where the location of the transition depends on the time over which the society is observed). If the value of δ of a society can be determined by fitting the model (with $\alpha = 0$) to a proxy for the society's status distribution, then the corresponding equi- σ line may provide an indication of the maximum level of authoritarianism over a particular observation time that can be tolerated by the society while maintaining essentially the same status distribution. This maximum level of authoritarianism would be reached when the equi- σ line intersects with the boundary separating regions II and III in Fig 10.

The original (two-parameter) version of our model is sufficient to fit the Canadian household income distribution. However, there is evidence that income distributions from many countries have a low-to-middle-income part that is well described by a distri-

bution function containing an exponential decay, and a separate, high-income part that decays more slowly [7, 43]. The inset of Fig 13 shows the Canadian household income distribution and the model-generated status distribution on a log-linear scale, in order to allow inspection of the large- S tail. The expected slower-than-exponential decay of the upper-tail is not seen in this data (for comparison, see the USA household income distributions plotted in Fig 14 below). This is most likely due to the fact that upper income cutoffs were applied to the public-use dataset by Statistics Canada, for the purpose of protecting confidentiality [44]. For this reason, only the lower-part of the Canadian income distribution is useful for the purposes of comparing the model results to real-world societies.

4.2 USA income distribution

Fig 14 shows United States household income distributions for the years 1990, 2000, and 2015 [45]. The USA datasets are 1-in-100 national random samples of the population. Dollar values for each of the three datasets have been adjusted to 1999 values in order to permit a comparison across time. In these distributions, the presence of an approximately exponentially-decaying lower-part (initial straight-line decrease in the inset of Fig 14 beginning after the peak at $S \approx 0.04 \times 10^6$), separated from a more slowly-decaying upper-tail is visible. The “break” point between the lower and upper parts of the data is present for all three curves and can be seen in the inset of Fig 14 at $S \approx 0.25 \times 10^6$. This break is observed in the income distributions of many different countries [7, 43].

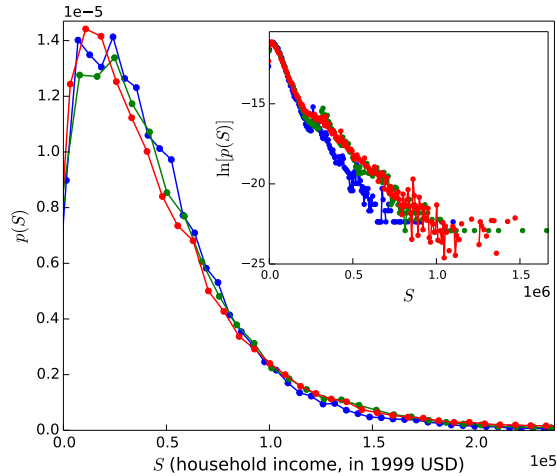


Fig 14: USA household income distribution as a function of time. USA household income distributions for three different years (blue: 1990; green: 2000; red: 2015). Dollar values have been converted to 1999 values to allow comparison of the different datasets [46]. A “break” in the data separating the high-income tail from the low-to-middle part of the income distribution can be seen in the inset at $S \approx \$250,000$. High-income cutoffs have been applied to the American data by the governmental agency that provided the data, causing the plateau in $\ln[p(S)]$ (inset) for the highest income values.

Several analyses of personal income distributions have found that the low-to-middle-income part of the distribution decays exponentially and that the high-income tail decays like a power-law [7, 43]. Based on these analyses, various econophysics models have been proposed with the goal of generating distributions of income with two-part shapes in which the lower-to-middle part of the income distribution follows an exponential distribution, and the upper tail follows a power-law distribution [29, 47, 48]. Among the models that generate a distribution of income or wealth as a self-organizing process based on interactions between individuals, several are able to produce either a power-law decay in the upper tail, or an exponential decay in the lower part of the distribution, but not both. The status distributions produced by the original (two-parameter) version of our model do not have two-part structures, and therefore never contain a “break” in the large- S tail similar to that seen in the inset of Fig 14. But the extended version of our model can produce two-part structures, as shown in section 3.6, where both the regime leading up to and the regime following the “break” decay exponentially.

4.2.1 Comparison with extended model distributions

Fig 15 shows the 2015 USA household income distribution and a simulated distribution. The inset (logarithmic scale on the y-axis) shows a break mirroring that of the actual data. The value of η was chosen such that $\eta\bar{S} = S_B$, where S_B is the location of the “break” point in the data, estimated from the data to be at \$275,000.

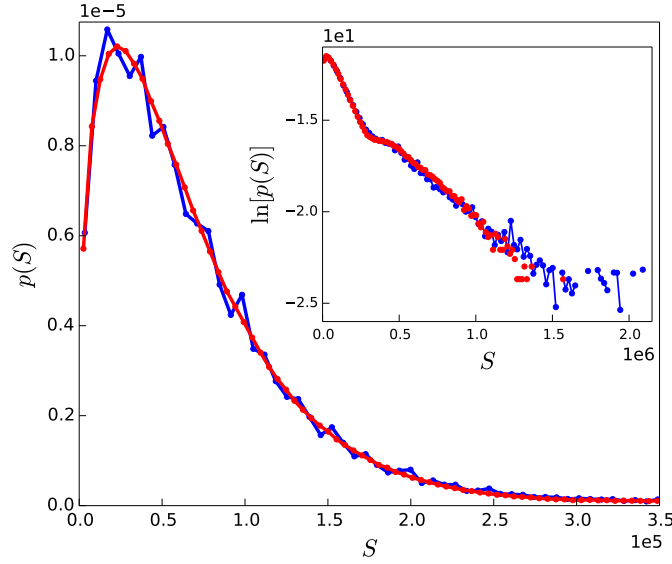


Fig 15: Fit of extended model status distribution to USA household income distribution. Simulated distribution (red curve) with parameters $\delta = 0.4$, $\alpha = 0$, $\eta = 3.5$, $\epsilon = 0.08$ compared to the distribution of USA household incomes from the year 2015 (blue curve).

Changes to the value of ϵ result in a poorer fit (see Appendix S2.A). As expected, ϵ is small, such that only 8% ($\epsilon = 0.08$) of fights that would not occur according to the threshold criterion do occur. Fig 15 shows that simulation of the extended model captures the main features of the 2015 USA household income data, including the “break” between the low-to-middle-income and upper-income parts of the distribution.

Several econophysics studies have found power-law distributions in the high-income tail of personal income distributions [7, 43]. However, a graphical analysis (Fig 16) comparing best fits of exponential and power-law distributions to the high-income tails of the 2000 and 2015 USA household income distributions shows that the household income data that we use as a proxy for societal status is not consistent with a power-law distribution but is consistent with an exponential distribution over large ranges. This is also confirmed by Kolmogorov-Smirnov tests for both distribution types. Further details are provided in Appendix S2.B [49–52].

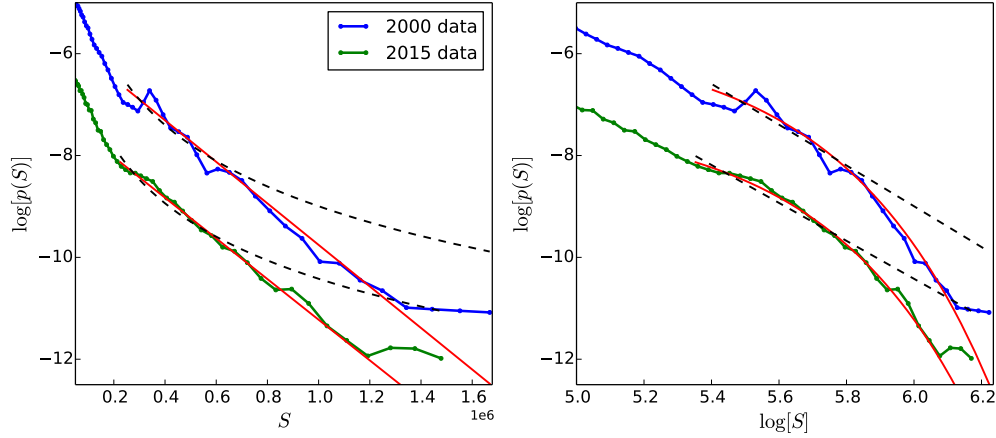


Fig 16: Functional form of high-income tail of USA household income distribution. Power-law (dashed black line) and exponential (solid red line) distributions with lower and upper bounds on the fitted distribution chosen to correspond to the full high-income tail. S represents USA household income data in 1999 USD. The curves for 2015 have been shifted down in the plots for better visualization.

In Fig 15, we have shown that our model, which is based entirely on interactions between individuals, and which does not require any exogenous influence such as redistribution by taxation, is able to produce a stable distribution that captures the main features of the two-part USA household income distribution. In order to accomplish this, it was necessary to establish limits about who can fight with whom, based on the statuses of the potential combatants. A simple threshold rule isolating high-status individuals from fights with low-status individuals, but which also permits infrequent exceptions to the threshold criterion, produced a simulated distribution with distinct lower and upper parts resembling those of the proxy distribution. Other ways to restrict the pairwise interactions between competing individuals lead to quantitatively similar behavior (see Appendix S2.C). In the status distributions generated by the extended model (section

3.6) individuals at the top-end of the distribution are typically separated from each other by amounts of status larger than the threshold amount $\eta\bar{S}$. This prevents many fights that would otherwise occur between such high-status individuals. A simple, additional extension to the model that allows all individuals with statuses greater than $\eta\bar{S}$ to interact with each other is included in Appendix S2.C.1, and shows an improved fit to the proxy data.

5 Conclusion

We have presented a simple model of the formation and evolution of social hierarchy, based solely on interactions (fights) between individuals that result in the transfer of status from the loser of the fight to the winner. We showed that the model exhibits regions in parameter-space in which the asymptotic distributions of status produced by the model either show a continuous unimodal behavior or take on a degenerate form, in which a single individual possesses all of the society’s status. In the latter case, intermediary distributions are long-lived for small positive values of the model parameters.

Our model suggests that there are two fundamental characteristics of status-determining interactions in a society – the level of intensity of interactions (δ) and the degree of authoritarianism (α) – that determine both the outcomes of the interactions and whether the society’s structure will be preserved for long times before undergoing eventual deterioration. These two parameters together with the parameters restricting the interactions between individuals control the shape of the (intermediary) status distribution, which becomes more unequal (larger standard deviation) as either α or δ is increased.

The presence of a characteristic time scale controlling the longevity of the intermediary distributions suggests a limit on the extent to which societal inequality can increase before a runaway deterioration occurs. Whether such a runaway occurs in real societies might depend on how this characteristic time scale compares with other, external time scales neglected in our model, such as the rate at which the society experiences external perturbations including wars with other societies, or major environmental changes.

Our model can also produce stable and long-lived status distributions which have identifiable low-to-middle and upper status regions, as occurs in advanced animal societies. The status distributions show good agreement with the distribution of household incomes in the USA, which we used as a proxy for societal status. This appears to be the first model in which the two-part structure of the proxy distribution emerges by self-organization based solely on interacting individuals.

A necessary foundation for more advanced studies of social hierarchy is the exploration of the simplest possible realistic models, including the determination of their limits. This was the goal of the present article. Future, network-oriented models may incorporate features such as the histories of interactions between individuals and cooperative behaviours including the formation of coalitions [30, 53–55] and mobbing [56, 57]. Such models may provide deeper understanding about the origins and evolution of societal structures, including the mechanisms responsible for societal destabilization or collapse.

Appendix S1

S1.A Comparison of simulation results to Ispolatov et al. analytic solution

In order to demonstrate that the definition of time as $t = 2t'/N$ in the simulation corresponds to the definition of time in the analytical solution of Eq 2 of the main text, we show (Fig 17) a plot of $M_2(t)$ when the parameter $\alpha = 0$ with time defined as $t = 2t'/N$. Each cluster of curves in the figure corresponds to a particular value of the model parameter δ . Within a single cluster of curves, simulation results are shown for three different system sizes, N . The red line shows a fit of Eq 4, where the fit parameters τ_1 and c_1 are equal to their corresponding analytic values from Eq 2. For example, for $\delta = 0.8$ and $\bar{S} = 1$, the fit parameters are $c_1 = 4.00$ and $\tau_1 = 6.29$, whereas Eq 2 gives $\hat{c}_1 = 4$ and $\hat{\tau}_1 = 6.25$.

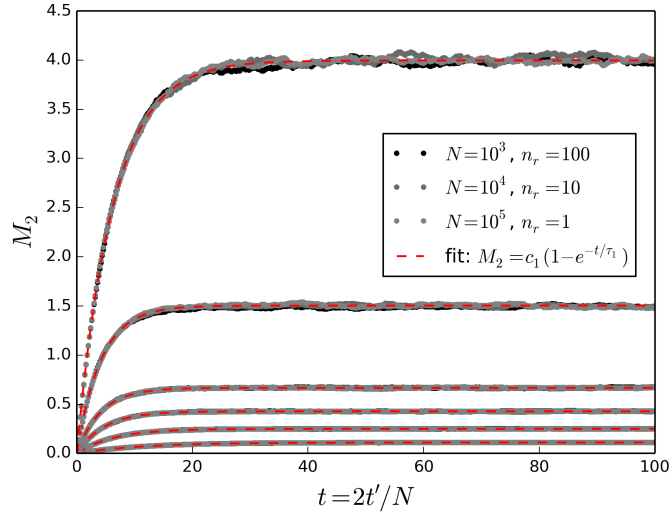


Fig 17: Evolution of $M_2(t)$ for $\alpha = 0$ and various values of δ (from bottom, $\delta = 0.1, 0.2, 0.3, 0.4, 0.6, 0.8$). Time is scaled so that $t = 2t'/N$. Fits are for $N = 10^5$. Data averaged over n_r realizations of the simulation.

S1.B Time evolution of distributions beginning from uniform initial condition

Figures showing the evolution of the model beginning from a uniform initial condition are included below, for the same values of δ and α shown in Figs. 2 and 4 of the main text. In the uniform initial condition, the initial status of each individual is chosen randomly from a uniform distribution with average status $\bar{S} = 1$. The time evolution beginning from this initial condition is qualitatively the same as for the egalitarian initial condition shown in Figs. 2 and 4 of the main text.

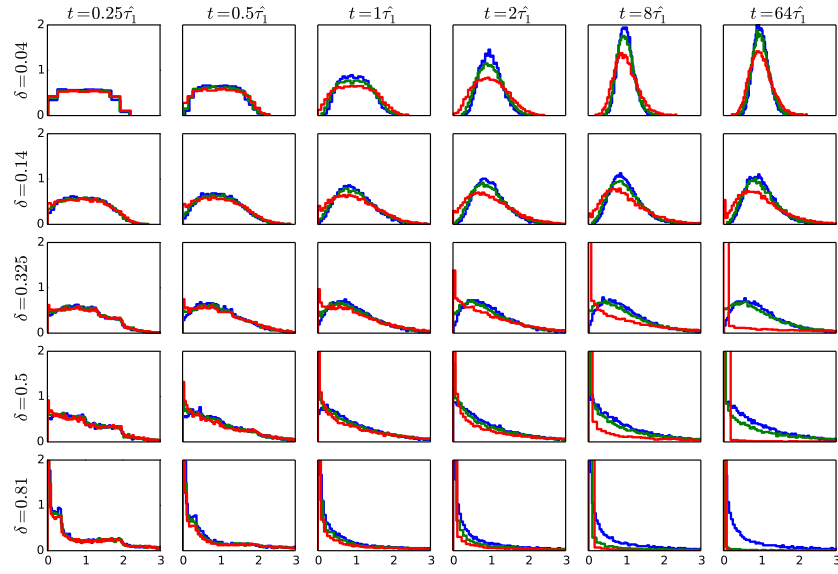


Fig 18: Time evolution of distributions for different values of δ , with $\alpha = 0$ (blue), $\alpha = 0.2$ (green), and $\alpha = 0.5$ (red), starting from an initial condition in which status is uniformly distributed (“uniform initial condition”). $N = 10^3$, $n_r = 20$.

S1.C Behaviour of τ_1 and τ_2 as a function of system size, N

In order to examine the behaviours of the characteristic times τ_1 and τ_2 as a function of system size, N , plots of $M_2(t)$ for different system sizes are shown in Fig 19. The parameters controlling the early-time behaviour of M_2 (c_1 and τ_1) remain constant as system size, N , is increased. The parameters controlling the long-time behaviour of M_2 increase linearly with N . For example, for $\alpha = 0.5$, the values of τ_2 extracted from a fit of Eq 6 are 1.17×10^5 , 1.18×10^6 , and 1.21×10^7 for system sizes $N = 10^2$, 10^3 , and 10^4 , respectively. Likewise, the parameter c_2 , which represents the “upper plateau” end-state value of M_2 increases linearly with N in the large- N limit (Eq 5).

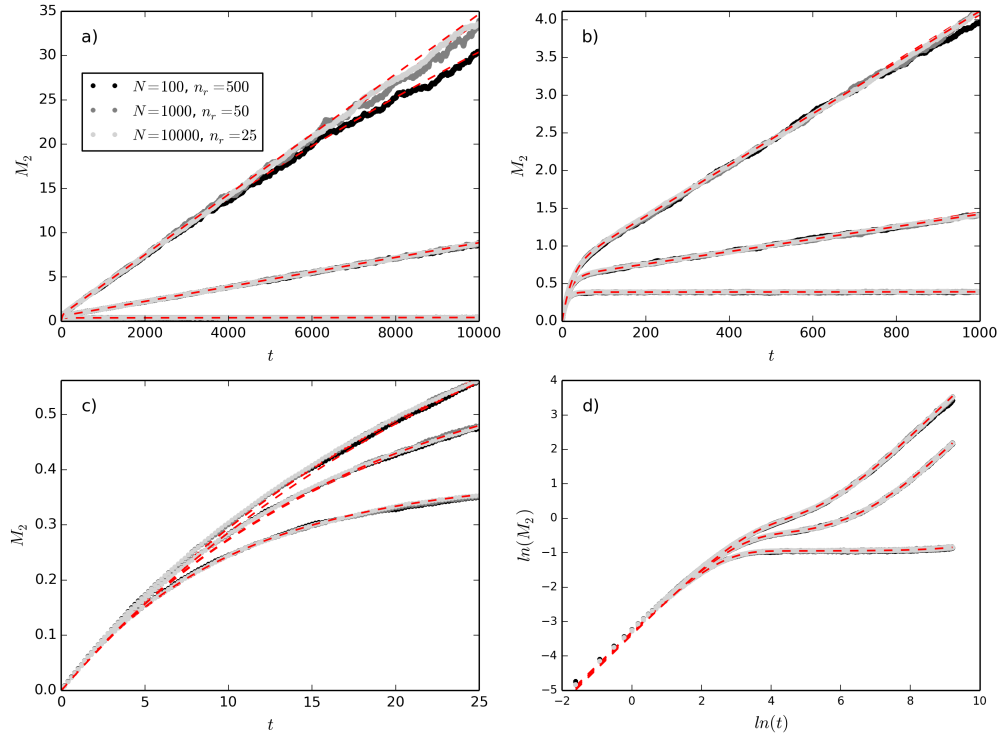


Fig 19: Evolution of $M_2(t)$ for $\delta = 0.2$ and $\alpha > 0$ (from bottom, $\alpha = 0.3, 0.5, 0.6$) for different system sizes N . (a)-(c) different (linear) scales on x and y axes. (d) log-log scale. Fits are of Eq 6 (red dashed lines) to simulated data.

S1.D Proof that N^2 fights are required to reach end-state when $\delta = 1$ and $\alpha = \infty$

In order to explore how the long-time behaviour of the evolution of the status distribution depends on system size N , we consider the extreme scenario of a system in which the higher-status individual in each fight wins with probability $p = 1$, and in which the winner of each fight receives all of the loser's status, leaving the loser with zero status. This extreme scenario corresponds to $\delta = 1$ and $\alpha = \infty$. In the model presented in the main text, δ is strictly less than 1, meaning that no single individual can ever possess all of the societal status of the system. However, in the following we set $\delta = 1$ in order to allow the system to obtain (after a finite time and for a finite system size) the end-state in which a single individual possesses all of the societal status and all other individuals have zero status. This simplifies the analysis, leading to the proof described below.

The goal of this exercise is to determine the time, τ_{end} , required to reach the totalitarian end-state beginning from an egalitarian initial condition. To do so, we will work backwards from the totalitarian end-state, in which a single individual possesses all of the societal status.

Working backwards from the end-state, we can consider the sequence of events that were required to arrive at the end-state. The first required event, working backwards, is a fight between two individuals possessing non-zero status. Since $\delta = 1$, one of these individuals loses and exits the fight with status equal to zero. The other individual wins the fight and receives all of the status of the loser, which, added to its pre-fight status, equals the total status of the system. Therefore, the end-state is preceded by a configuration of the system in which only two individuals possess non-zero status. The probability that these two particular individuals are selected to fight each other is the probability of selecting the first individual OR the second individual AND the probability of selecting the remaining individual:

$$\rho_2 = \left(\frac{1}{N} + \frac{1}{N} \right) \frac{1}{N-1} = \frac{2}{N(N-1)}. \quad (9)$$

Continuing to work backwards, in order to obtain the configuration of the system in which there are two individuals with non-zero status, a preceding configuration having three individuals with non-zero status is required. The probability that two of these three individuals are selected to fight is:

$$\rho_3 = \binom{3}{2} \frac{2}{N(N-1)}. \quad (10)$$

Following through with this logic, we find $\rho_N = \binom{N}{2} \frac{2}{N(N-1)}$. Now, the expected number of fights that will elapse between the required configuration k and the subsequent required configuration $k-1$ in this sequence is ρ_k^{-1} . Therefore, the expected number of fights to reach the end-state is:

$$\begin{aligned}
\tau'_{end} &= \frac{N(N-1)}{2} \left(\frac{1}{\binom{2}{2}} + \frac{1}{\binom{3}{2}} + \frac{1}{\binom{4}{2}} + \dots + \frac{1}{\binom{N}{2}} \right) \\
&= N(N-1) \sum_{k=2}^N \frac{1}{k(k-1)}.
\end{aligned} \tag{11}$$

The sum in Eq 11 approaches 1 for large N , such that $\tau_{end} \approx N^2$. The time to reach the end-state when $\delta = 1$ and $\alpha = \infty$ is therefore $\tau_{end} \approx 2\tau'_{end}/N = 2N$, for large N .

This proof is included as a demonstration of the configurational reasons why the long-time (approach to the end-state) evolution of the model dynamics increases in proportion to the system size N .

S1.E Phenomenology of the time-evolution of status distributions when $\alpha > 0$

In this section we provide some additional details about the phenomenology of the evolution of the status distributions when $\alpha > 0$. Fig 20a shows a plot of $M_2(t)$ for a system with $N = 1000$, $\delta = 0.2$, and several values of α .

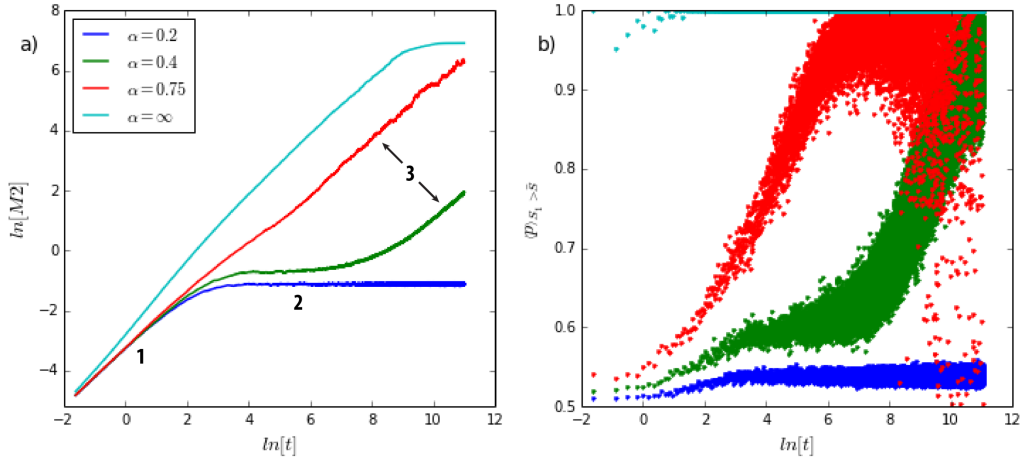


Fig 20: (a) $M_2(t)$ on a log-log scale, with four stages of evolution indicated. $\delta = 0.2$ for all curves. (b) Probability p (averaged over preceding 100 fights, considering only those fights in which $S_1 > \bar{S}$) as a function of time. $N = 1000$ (a and b) and $n_r = 10$ (a) and $n_r = 1$ (b)

Three distinct stages in the evolution of $M_2(t)$ can be identified, as indicated on the log-log plot of $M_2(t)$ shown in 20a. First (stage 1), there is a rapid change away from the initial condition into a distribution similar in shape to the $\alpha = 0$ (true steady-state) distribution. This distribution shape is essentially maintained during stage 2, such that

$M_2(t)$ changes only very slowly with time. For example the curve corresponding to $\alpha = 0.2$ (blue) in Fig 20a remains in stage 2 over the time scale of the simulation (to demonstrate this, distributions corresponding to specific points in time along this curve are shown in Fig 21). The duration of stage 2 decreases with increasing α , as can be seen in the curve corresponding to $\alpha = 0.4$ (green) in Fig 20a (distributions corresponding to specific points in time along this curve are shown in Fig 22). When α is increased further, stage 2 essentially disappears (red curve in Fig 20a – distributions corresponding to specific points along this curve are shown in Fig 24).

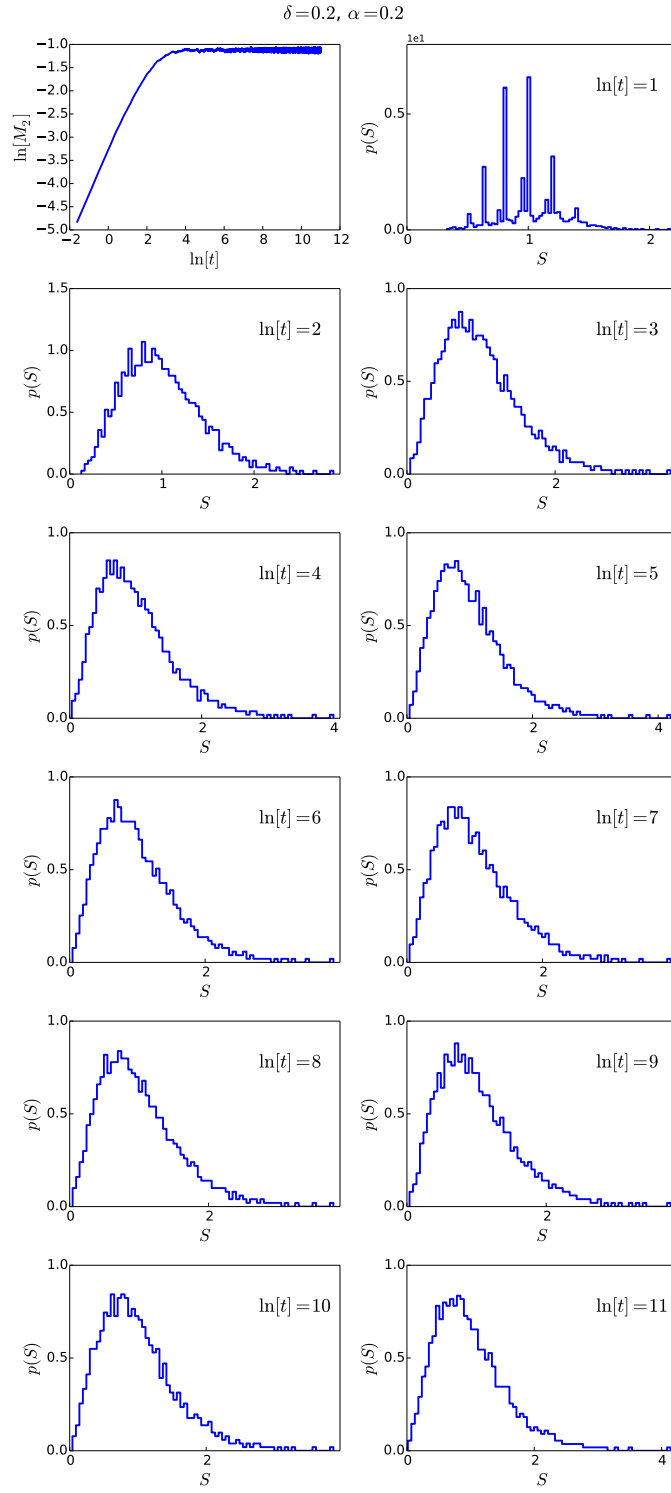


Fig 21: Time evolution of distributions for $\delta = 0.2$, $\alpha = 0.2$. $N = 1000$, $n_r = 10$.

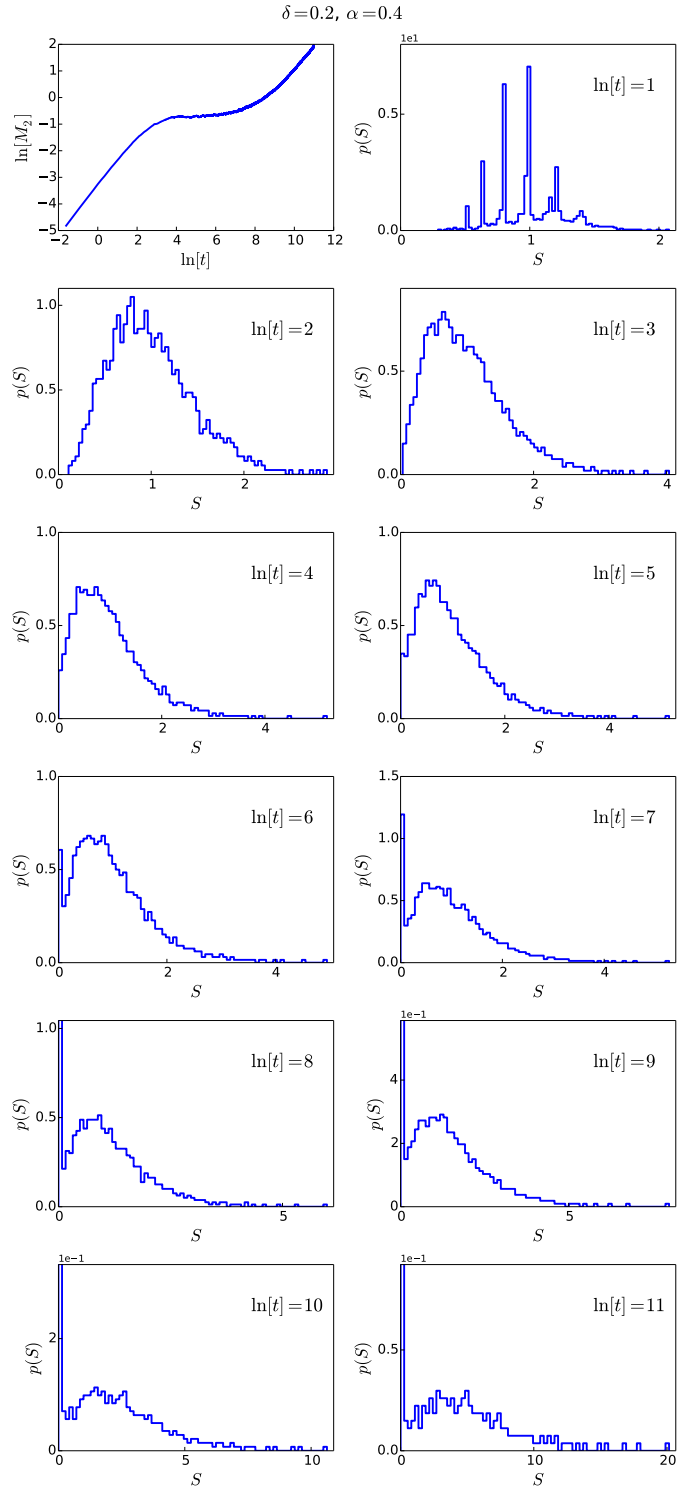


Fig 22: Time evolution of distributions for $\delta = 0.2, \alpha = 0.4$. y-axis scale adjusted in plots for $\ln[t] = 8$ to 11 to allow visualization of large- S range of distribution. $N = 1000$, $n_r = 10$.

Transitioning from stage 2 to stage 3, the distribution accumulates many individuals with very low statuses, and several higher-status individuals emerge. Stage 3 then consists of the slow evolution of this highly skewed distribution. A particular characteristic of stage 3 is that, for fights involving at least one individual who still retains sizeable status (e.g., $S_1 > \bar{S}$), the probability $p \rightarrow 1$. This is illustrated in Fig 20b, in which p is averaged over the preceding 100 fights, considering only those fights in which $S_1 > \bar{S}$, giving the quantity $\langle p \rangle_{S_1 > \bar{S}}$. The fact that $\langle p \rangle_{S_1 > \bar{S}} \rightarrow 1$ signifies that the higher-status individual in any given fight (excluding fights in which neither individual has greater than average status) is virtually guaranteed to win. For finite values of $\alpha > 0$, in order for this to occur, there must be a large relative status between the two individuals. Stage 3 is therefore characterized by a distribution in which the ratio of S_2/S_1 for any two randomly-selected individuals is small enough such that $\langle p \rangle_{S_1 > \bar{S}} \rightarrow 1$ for fixed α (as per Eq 1). The large-time decrease in $\langle p \rangle_{S_1 > \bar{S}}$ (e.g. for the red curve corresponding to $\alpha = 0.75$ in Fig 20b, at $\ln[t] = 8$ to $\ln[t] = 11$) occurs as individuals with $\bar{S} < S < S_H$ begin to experience decreases in status. Here, S_H is the status of the highest-status individual. This is illustrated in Fig 23, which plots the sum of statuses of all individuals with $\bar{S} < S < S_H$ as a function of time.

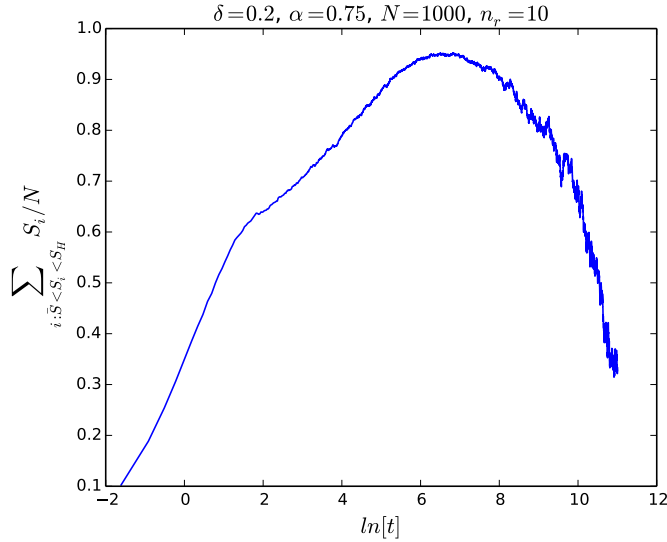


Fig 23: Sum of statuses of all individuals with $\bar{S} < S < S_H$ vs. t , for $\delta = 0.2$ and $\alpha = 0.75$. $N = 1000$, $n_r = 10$.

The transition from stage 3 to the totalitarian end-state involves the decrease in the sum of statuses shown in Fig 23 following the maximum at $\ln[t] \approx 7$. This shows that in its evolution toward the end-state, the distribution must pass through a series of configurations (stage 3) in which there are a number of individuals with higher-than-average statuses, these individuals having extracted their large statuses from the mass of very low status individuals that accumulates in the transition from stage 2 to stage 3. Only after stage 3 has been obtained are the conditions present in which fights between

high status individuals can lead to the emergence of a single dominant individual, in the end-state.

In the end-state, virtually all individuals have $S \approx 0$, except for a single dominant individual with status approaching the total status of the system, such that $S_H \rightarrow N\bar{S}$ and $M_2(t) \rightarrow c_2$. The fourth (light blue) curve in Fig 20 corresponds to $\alpha = \infty$, signifying that the higher-status individual in any fight is guaranteed to win (several points in Fig 20b for which $\langle p \rangle_{S_1 > \bar{S}} < 1$ for this curve result from fights in which $S_1 = S_2$ due to the egalitarian initial condition). Distributions at specific points along this curve are shown in Fig 25.

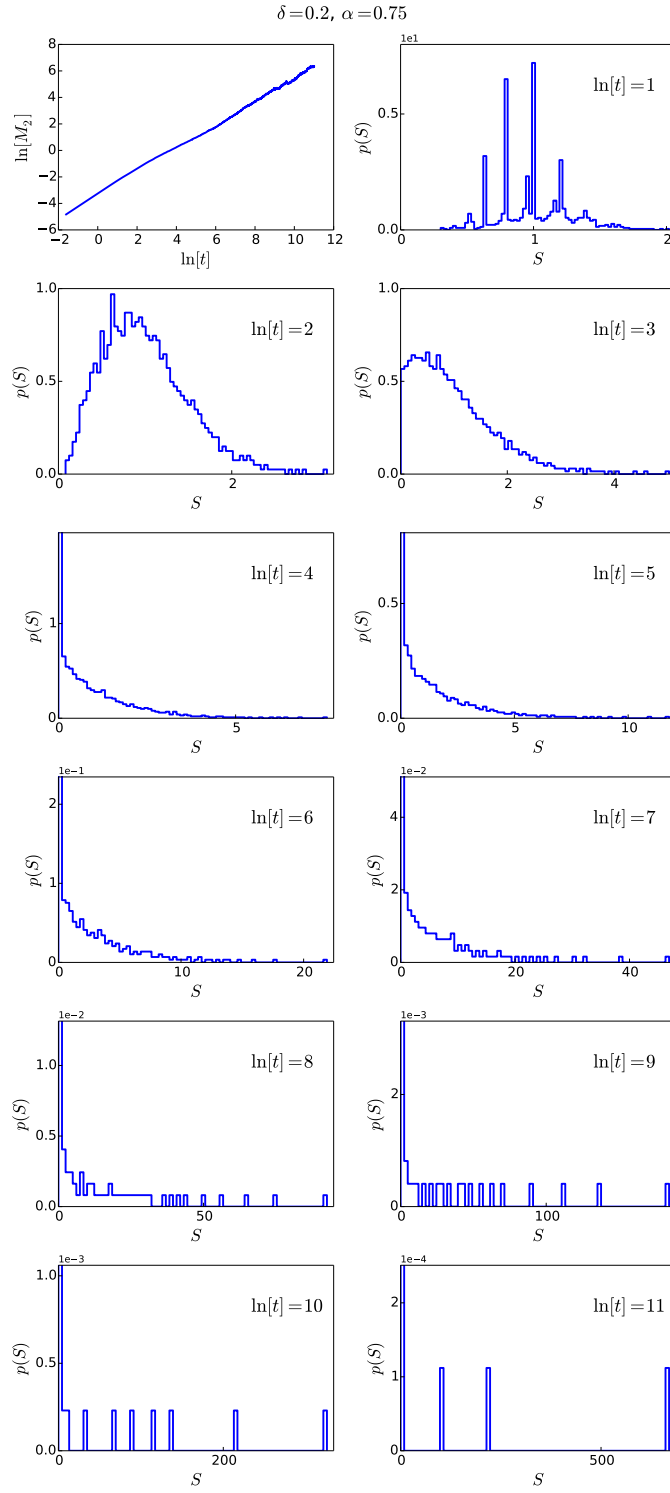


Fig 24: Time evolution of distributions for $\delta = 0.2, \alpha = 0.75$. y-axis scale adjusted in plots for $\ln[t] = 4$ to 11 to allow visualization of large- S range of distribution. $N = 1000$, $n_r = 10$.

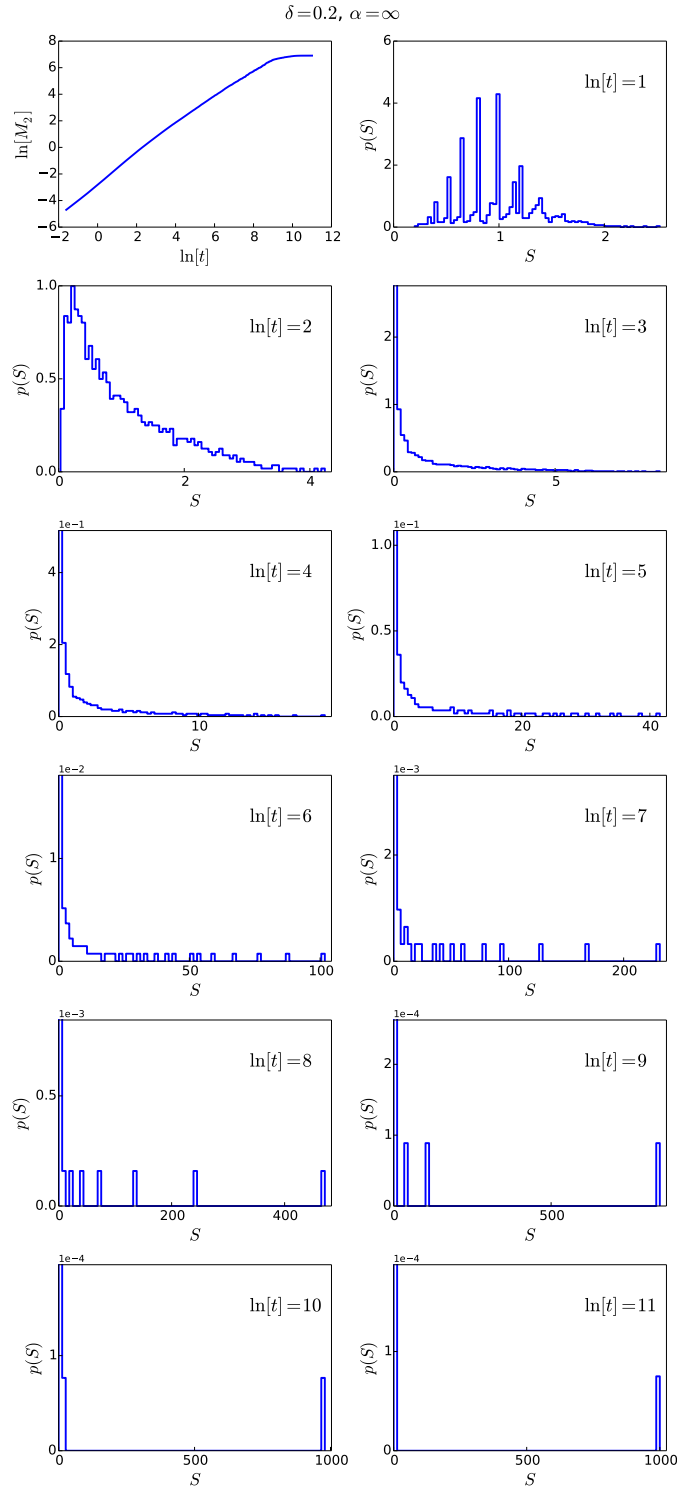


Fig 25: Time evolution of distributions for $\delta = 0.2, \alpha = \infty$. y-axis scale adjusted in plots for $\ln[t] = 3$ to 11 to allow visualization of large- S range of distribution. $N = 1000$, $n_r = 10$.

Lastly, a plot showing the same quantities as in Fig 20, but where α is fixed and δ is varied, is included below for comparison. As can be seen, as δ is increased, the duration time of stage 2 decreases.

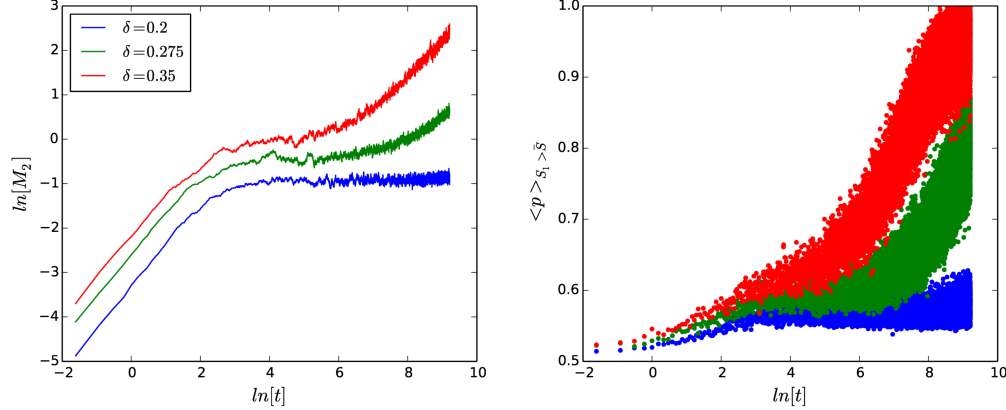


Fig 26: (a) $M_2(t)$ on a log-log scale. (b) Probability p (averaged over preceding 100 fights, considering only those fights in which $S_1 > \bar{S}$) as a function of time. $\alpha = 0.3$ for all curves. $N = 1000$, $n_r = 10$.

S1.F Proof that a single individual with non-negligible status remains in the totalitarian end-state

When $\alpha > 0$, the system approaches an end-state in which a single individual possesses virtually all of the society's status and all other individuals have status approaching zero. An argument that only a single individual with non-negligible status remains in the end-state (and not, for example, multiple high-status individuals), is as follows.

Consider a large (but finite) system of N individuals. When $\alpha > 0$, beginning from an egalitarian initial condition, the system evolves such that there are relatively few individuals with large status and relatively many individuals with small status (see section S1.E). Since the average status of the system is constant, we can use it as a reference point to define “large status” to mean greater than average status, and “small status” to mean less than average status. The subsequent dynamics can be understood in terms of two timescales. The first timescale, λ_1 , sets the time (measured in number of fights) that transpires, on average, between fights involving the same two particular individuals. Since pairs of individuals are picked randomly from among the population, λ_1 is determined by the system size N and remains unchanged as the system evolves.

The second timescale, λ_2 , relates to the time required for an individual with less than average status to achieve an upset victory over an individual with greater than average status. Once the system has evolved to a point in which there are few individuals with high statuses and many individuals with low statuses, such an upset is the only way in which an individual with lower than average status can obtain greater than average status. λ_2 is determined by the average probability, $\langle p_{upset} \rangle$, with which an upset occurs

(the smaller $\langle p_{upset} \rangle$, the larger λ_2). The probability for such an upset to occur (in any particular fight) is less than 50%, by Eq 1 of the main text. Therefore, fights that involve one individual with greater than average status and one individual with less than average status will generally result in a transfer of status from the lower-status individual to the higher-status individual. This creates a net transfer of status from individuals with lower than average status to individuals with greater than average status. One outcome of this net transfer of status is a reduction in $\langle p_{upset} \rangle$. Consequently, the timescale λ_2 must increase with time (number of fights).

Since λ_1 remains constant whereas λ_2 increases as the system evolves, eventually λ_1 dominates the dynamics such that any two particular individuals fight one another much more frequently than any one particular individual with lower than average status achieves an upset that transforms it into an individual with greater than average status. Since fights between any two particular high-status individuals occur with higher frequency than fights in which a low-status individual achieves an upset over a high-status individual, there is a net flow of the losers of fights between two high-status individuals into the ranks of those with lower than average status.

The rate at which this net flow of losers occurs increases as λ_2 increases, and after an infinite number of fights ($t \rightarrow \infty$), only a single individual with greater than average status remains.

S1.G Technical aspects regarding τ_2 extraction and errors

For small values of α , τ_2 diverges, such that very long simulations are required in order to evaluate τ_2 . In order to simplify matters, we consider a linear expansion of Eq 6 in the region where $\tau_1 \ll t \ll \tau_2$:

$$M_2 = c_1 + (c_2 - c_1)(1 - e^{-t/\tau_2}) \approx c_1 + \frac{c_2 - c_1}{\tau_2}t. \quad (12)$$

A linear fit to $M_2(t)$ data in the $\tau_1 \ll t \ll \tau_2$ can then be made, with intercept c_1 and slope $s = (c_2 - c_1)/\tau_2$. This allows τ_2 to be calculated, since c_2 is known from Eq 5.

An example is shown in Fig 27a. Here, a set of 10 realizations of the simulation were performed. The plot contains the 10 different $M_2(t)$ curves overlayed one top of each other, with a linear fit (red line) to the combined data for all 10 curves. Fig 27b shows the distribution of residuals. The residuals are skewed, such that large increases in M_2 are more likely than large decreases.

Propagation of errors shows that $\Delta \ln[N/\tau_2] \approx \Delta s/s$, assuming that $\Delta s \gg \Delta c_1$ (justified below). This means that as α is decreased and s approaches 0, it eventually becomes impossible to obtain a meaningful fitted value of τ_2 . Following this reasoning, we include points on the plot of $\ln[N/\tau_2]$ vs. α shown in Fig 7 for values of α for which $\Delta s/s < 1$.

Since $M_2(t)$ has a skewed (non-Normal) distribution of residuals and contains time-correlations, it is difficult to obtain a meaningful value of Δs from a regression. We therefore estimate Δs using uncorrelated, normally-distributed synthetic data with a width that is representative of the fluctuations in $M_2(t)$. This is done by generating random data from a Normal distribution with width equal to the average (over all time points) of the standard deviation taken, at each time t , across the 10 realizations of the simulation. An example of this synthetic data is shown in Fig 27b (black curve). A least squares fit provides a correct determination of the error on the slope and intercept of this synthetic data, which we use as estimates for Δs and Δc_1 . In this way, we see that $\Delta s \gg \Delta c_1$.

This procedure provides an estimate of the (small α) limit beyond which points cannot be added to the plot of Fig 7 (obtaining further points would require longer simulation times that are beyond the scope of this study). The procedure does not provide a reasonable estimate of error bars for Fig 7. However, $\Delta \ln[N/\tau_2]$ is expected to increase with decreasing α (since s decreases, while Δs remains approximately constant), and this is reflected in increased fluctuations of $\ln[N/\tau_2]$ about the straight black lines in Fig 7 as α decreases.

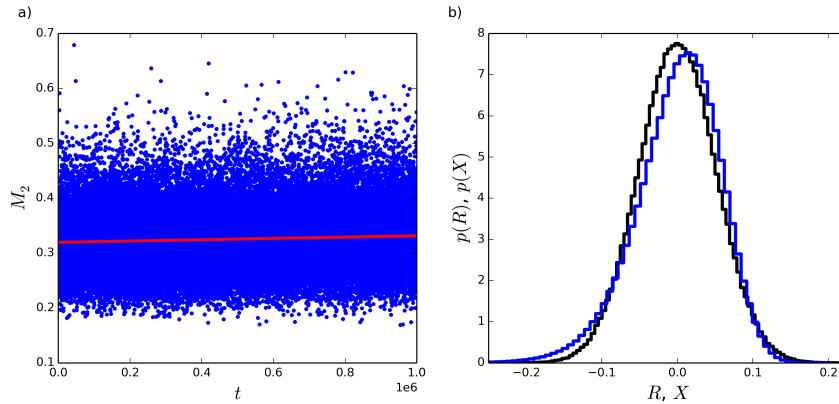


Fig 27: (a) 10 overlaid realizations of $M_2(t)$ for $\delta = 0.2$, $\alpha = 0.2$, $N = 100$, $n_r = 10$, and linear fit (red line). (b) Distribution of residuals $R = y_{fit} - M_2$ (blue curve) and a Normal distribution with width equal to $\langle \sigma(M_2(t)) \rangle$ of a random variable X (black curve).

S1.H Determining the location of the transition between regions II and III of Fig 10

S1.H.1 Using a criterion based on the slope of $M_2(t)$

The location of this transition between regions II and III of Fig 10 depends on the time, τ_{obs} , over which the system is observed (simulated). A simple criterion equates the onset of runaway with the appearance of a positive slope in the long-time portion of $M_2(t)$. Whether such a slope is observed in $M_2(t)$ depends on the size of the fluctuations in the simulation data. We ran $n_r = 25$ realizations of the simulation for system size

$N = 1000$. In order to determine if the system is in the long-lived state for a particular value of α , we first fit a straight line to $M_2(t)$ over a range $[t_0, \tau_{obs}]$, where $t_0 \gg \tau_1$ such that $M(t_0)$ is on the $M_2(t)$ plateau that follows the initial transient evolution away from the initial (egalitarian) distribution. The transition is considered to have occurred at the value of α for which the long-time part of the $M_2(t)$ curve increases by 2.5% over the observation (simulation) time τ_{obs} . For the choice of N and n_r used, this amount of increase corresponds to approximately 5 times the standard deviation of the residual $R(t) = \hat{M}_2(t) - M_2(t)$, where $\hat{M}_2(t)$ is the linear fit, and $M_2(t)$ is averaged over the $n_r = 25$ realizations. Therefore, the distribution is considered to be long-lived over the interval $[t_0, \tau_{obs}]$ as long as $m(\tau_{obs} - t_0) < 0.025b$, where m is the slope and b the intercept of the linear fit.

S1.H.2 Using the Arrhenius relation between τ_2 and α

The criterion (see above, section S1.H.1) of a 2.5% increase in $M_2(t)$, used to determine the location of the transition between the long-lived state and runaway, can be written in terms of Eq 6 as:

$$M_2(\tau_{obs}) = 1.025c_1 \approx c_1 + (c_2 - c_1)(1 - e^{-\tau_{obs}/\tau_2}), \quad (13)$$

where the approximation comes from the assumption that $\tau_{obs} \gg \tau_1$. Rearranging Eq. 13 in terms of τ_{obs} gives the following relationship:

$$\tau_{obs} \approx -\tau_2 \ln \left(1 - \frac{0.025c_1}{N - 1 - c_1} \right). \quad (14)$$

Now, we fix τ_{obs} and adjust α until the relationship in Eq. 14 is satisfied. Inserting the relationships $\alpha_b = 0.53\delta^{-1.21}$ (Fig 8) and $Nf_0 = \delta^{1.3}$ (Fig 9) into Eq 7 and rearranging, we find:

$$\begin{aligned} \alpha_t &\approx \frac{\alpha_b}{\ln[\tau_2(\alpha_t)f_0]} \\ &\approx \frac{0.53\delta^{-1.21}}{\ln \left[\frac{-\tau_{obs}\delta^{1.3}}{N \ln \left(1 - \frac{0.025c_1}{N-1-c_1} \right)} \right]}, \end{aligned} \quad (15)$$

where α_t is the location of the transition (as defined by the criterion stated above) and $\tau_2(\alpha_t)$ is the value of τ_2 when $\alpha = \alpha_t$.

A factor of c_1 appears twice in Eq. 15. While c_1 is in fact a function of δ and α , it changes slowly with α (Fig 6d). Therefore, we set c_1 to be equal to its value when $\alpha = 0$, such that $c_1 = \delta/(1 - \delta)$ (see Eq 2). With these assumptions in place, Eq. 15 produces the solid black ($\tau_{obs} = 10^4$) and red ($\tau_{obs} = 10^3$) curves in Fig 10.

S1.H.3 N -dependence of α_t

The N -dependence of α_t is contained within the denominator of the argument of the logarithm in the denominator of Eq. 15. Fig 28 shows a plot of this part of Eq. 15 as a function of N . The plot becomes effectively constant for large N , showing that the N -dependence of α_t vanishes for increasing N such that the location of the transition between the long-lived state and runaway effectively does not depend on system size.

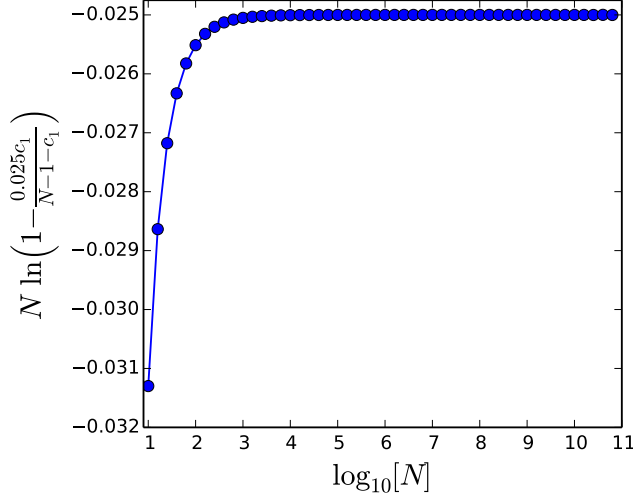


Fig 28: The part of Eq. 15 containing a dependence on N plotted vs. powers of N , and becomes effectively constant at large N .

S1.H.4 Alternative location of the transition between regions II and III according to Arrhenius relation

In some physical systems governed by an Arrhenius relation, the location of the operational transition between two regimes is taken by the researcher to be at the value of the control parameter (usually temperature, in physical systems) for which the transition rate τ is equal to the measurement time τ_m . This is the case in the blocking transition of superparamagnetism, for example [39].

We could use this reasoning to locate the transition between the long-lived state and runaway in our model at a value of $\alpha = \alpha_t^*$ for which $\tau_2 = \tau_{obs}$. Re-arranging Eq. 7 and substituting in the relationships for α_b and Nf_0 , we find:

$$\begin{aligned}
 \alpha_t^* &= \frac{\alpha_b}{\ln[\tau_{obs} f_0]} \\
 &= \frac{0.53\delta^{-1.21}}{\ln \left[\frac{1.03\delta^{1.3}\tau_{obs}}{N} \right]}.
 \end{aligned} \tag{16}$$

In a physical experiment, the criterion for setting the location of the operational transition is primarily determined by the measurement type. For some measurement types, it may be appropriate or natural to set the location of the transition at a value of the control parameter analogous to α_t^* . In our system, this would correspond to identifying the transition between the long-lived state and runaway at a value of α for which $M_2 = M_2(t = \tau_2) \approx c_2(1 - 1/e)$. This represents a significant evolution of the system toward the totalitarian end-state, which is not suitable for our purpose. Rather, our goal is to determine the value of α for which, on the scale of the observation time considered, the long-lived state plateau value of M_2 is lost and a noticeable increase in $M_2(t)$ is observed. We therefore place the location of the transition at α_t .

S1.I Additional details about evolution of extended model distributions

The figures in this section are included to show how the status distributions produced by the extended model (presented in section 2.1 of the main text) evolve in time. In the upper left panel of each figure, the evolution of $M_2(t)$ on a log-log scale is shown. The status distributions are shown at various points in time (indicated within the plots) in the remaining panels. For each figure, the simulation had system size $N = 1000$, and the results are averaged over $n_r = 5$ realizations of the simulation. The simulation parameters $\delta = 0.2$, $\eta = 1.0$, and $\epsilon = 0.1$ are fixed for all figures, and the parameter α is varied.

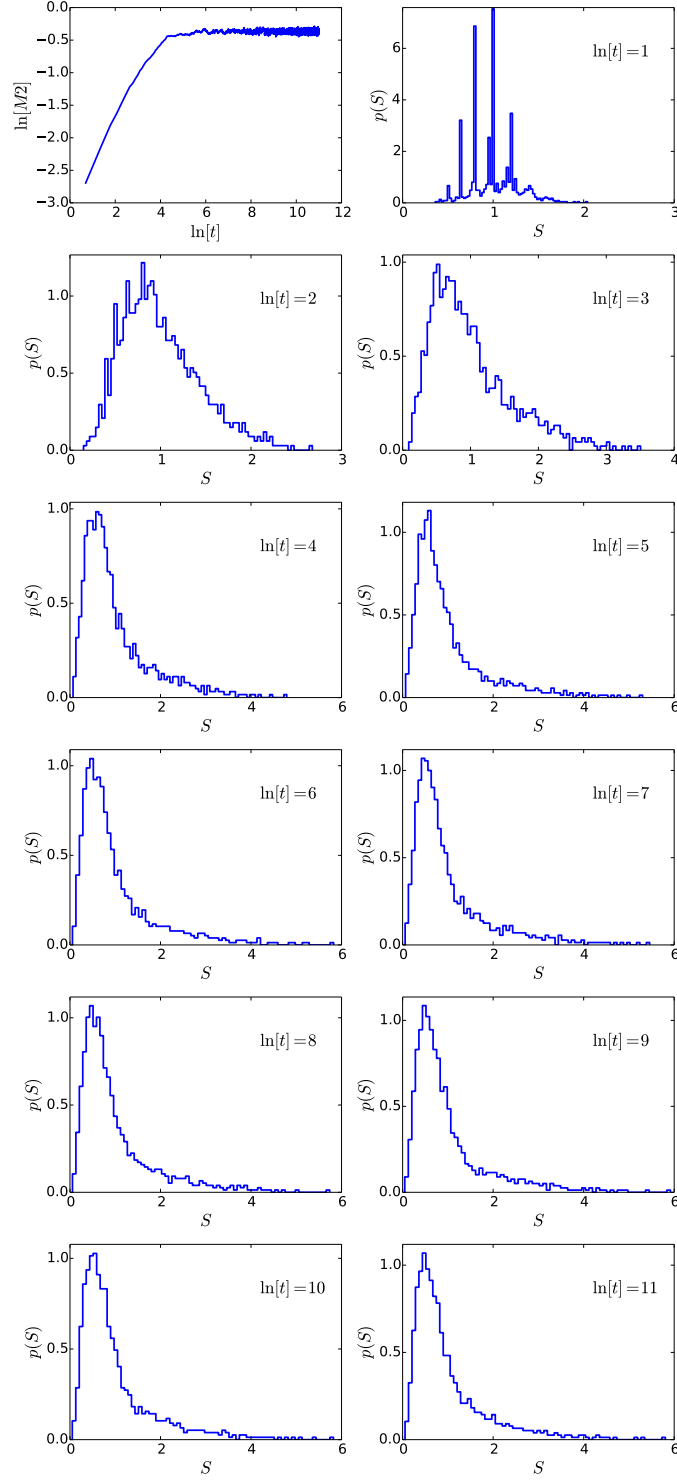


Fig 29: Time evolution of distributions for $\delta = 0.2$, $\alpha = 0.0$, $\eta = 1.0$, $\epsilon = 0.1$.

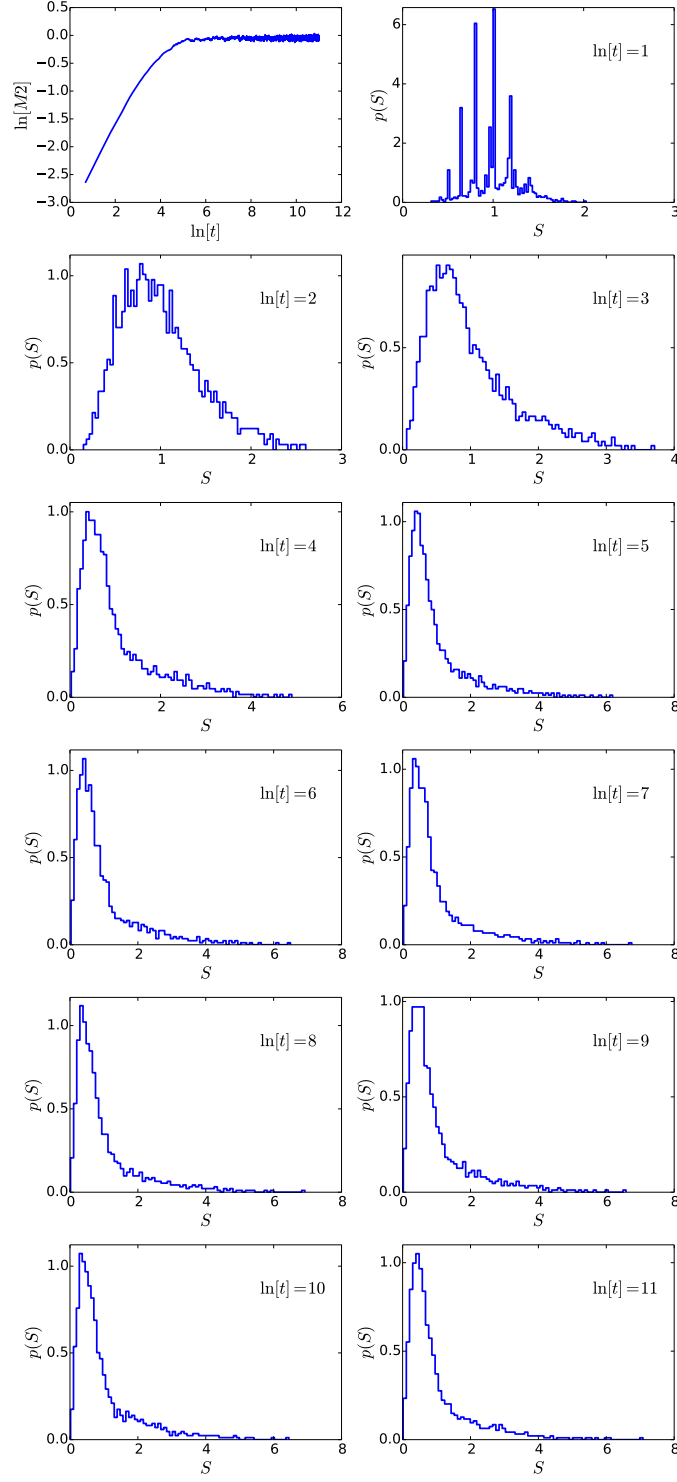


Fig 30: Time evolution of distributions for $\delta = 0.2$, $\alpha = 0.2$, $\eta = 1.0$, $\epsilon = 0.1$.

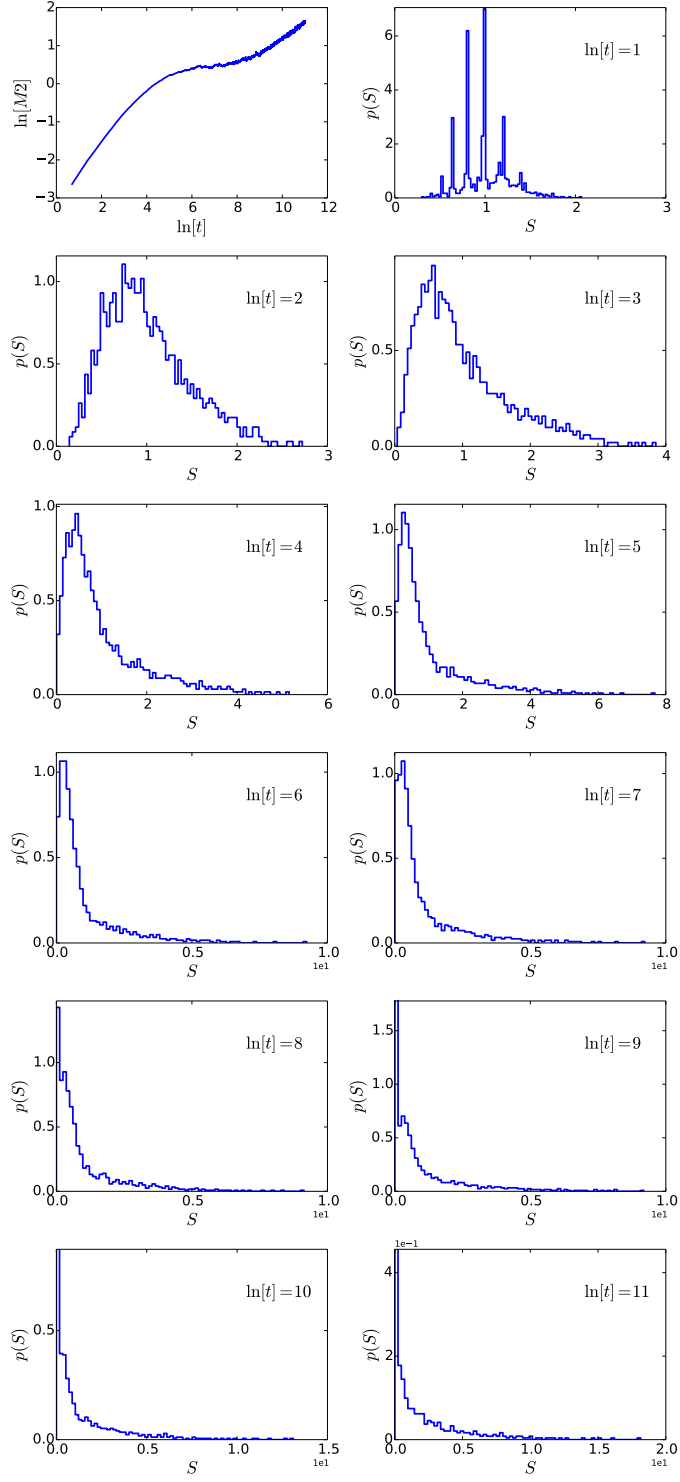


Fig 31: Time evolution of distributions for $\delta = 0.2$, $\alpha = 0.4$, $\eta = 1.0$, $\epsilon = 0.1$.

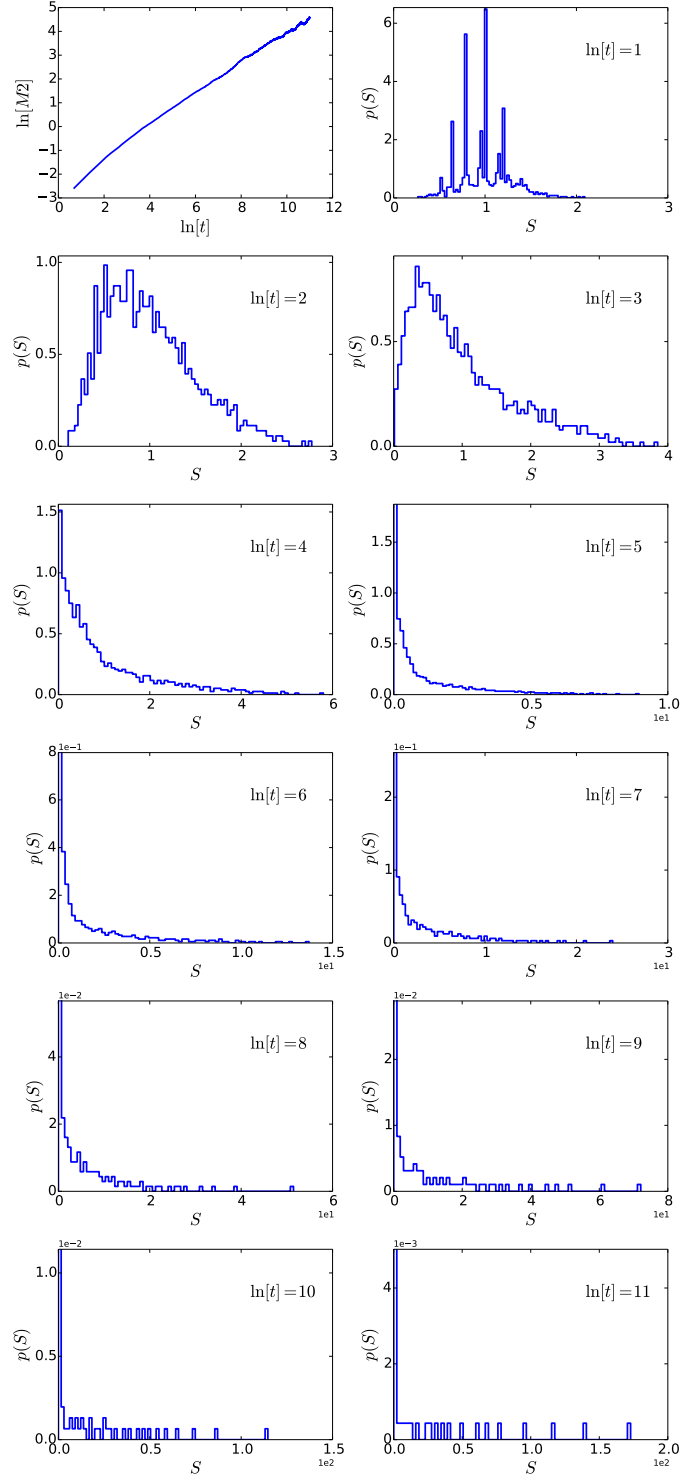


Fig 32: Time evolution of distributions for $\delta = 0.2$, $\alpha = 0.75$, $\eta = 1.0$, $\epsilon = 0.1$.

Appendix S2

S2.A Sensitivity of fit to USA income data to change in parameter ϵ

Fig 15 of the main text shows a fit of the extended model to the USA household income distribution. The parameter η is set such that $\eta\bar{S} = S_B$, where S_B is the “break point” in the data. The parameter ϵ in Fig 15 was chosen to be equal to 0.08 in order to obtain a good fit to the income data. Two figures are included below to show how decreasing (Fig 33) or increasing (Fig 34) the value of ϵ affects the fit to the proxy data.

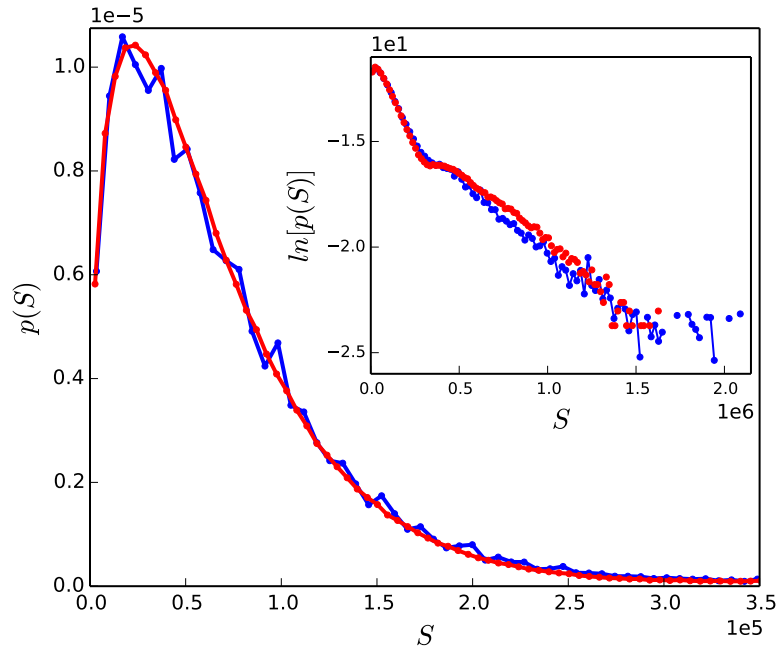


Fig 33: Fit of extended model ($\eta = 3.5$, $\epsilon = 0.06$) to 2015 USA household income data.

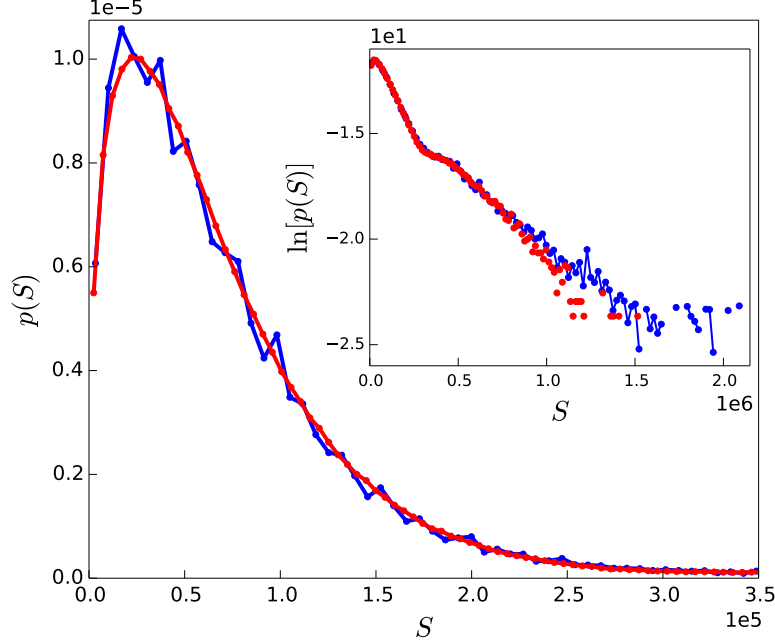


Fig 34: Fit of extended model ($\eta = 3.5$, $\epsilon = 0.1$) to 2015 USA household income data.

S2.B High-income tails of USA household income distributions

In Fig 16 of the main text, fits of exponential and power-law distributions to the high-income tail of the 2000 and 2015 USA household income distributions were shown. Normalized with respect to the boundaries S_l and S_h , the probability density function, $p(S)$, of the power-law distribution is:

$$p(S) = \frac{S_l^{1-\gamma} - S_h^{1-\gamma}}{\gamma - 1} S^{-\gamma}, \quad (17)$$

and that of the exponential distribution is:

$$p(S) = \frac{e^{(S_l - S)/T}}{T(1 - e^{(S_l - S_h)/T})}, \quad (18)$$

where the parameters γ and T are determined by maximum likelihood estimation using the data within the range $[S_l, S_h]$ [49]. Two additional figures showing different $[S_l, S_h]$ ranges are included below. As for Fig 16 of the main text, the black dashed line shows the power-law fit and the solid red line shows the exponential fit. The 2015 curves have been shifted down in the plots for better visualization.

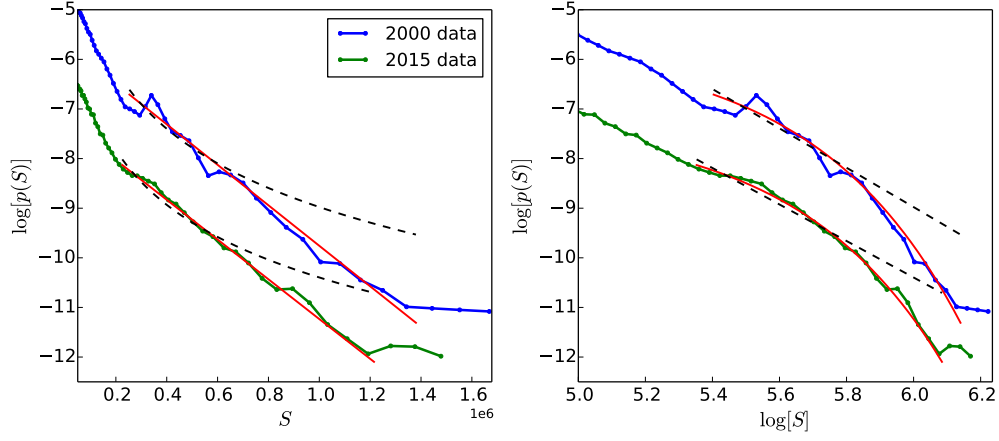


Fig 35: Power-law (dashed black line) and exponential (solid red line) distributions with S_l and S_h chosen to correspond to the high-income tail, excluding the highest-income points. For the fits to the 2015 data shown in this figure, the choice of S_h resulted in the exclusion of the 15 largest data points. For the fits to the 2000 data shown in this figure, the choice of S_h resulted in the exclusion of the two largest data points. Exclusion of the highest-income data points is justified because high-income cutoffs have been artificially applied to the USA data by the governmental agency that provided it, for the purpose of protecting confidentiality. S represents USA household income data in 1999 USD.

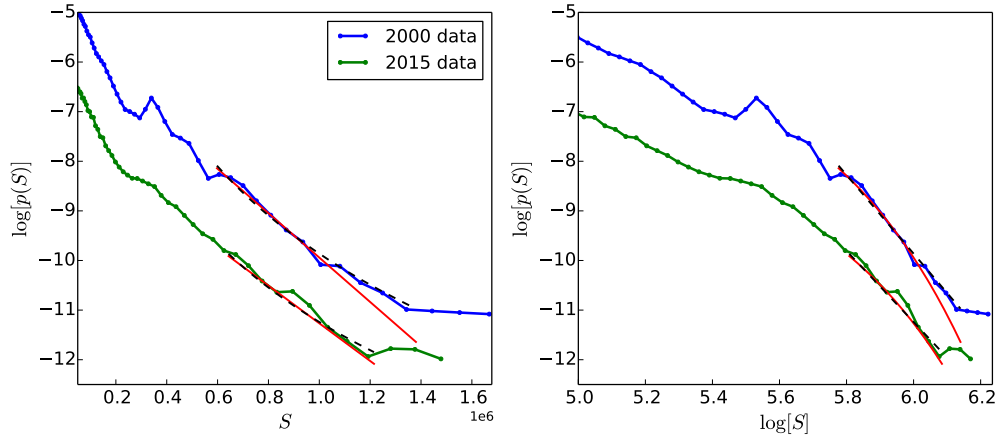


Fig 36: Power-law (dashed black line) and exponential (solid red line) distributions with S_l and S_h chosen to correspond approximately to the latter part of the high-income tail. Graphical analysis shows that, at best, a power-law can only fit segments of the high-income tail. S represents USA household income data in 1999 USD.

S2.B.1 Kolmogorov-Smirnov (KS) test

A Kolmogorov-Smirnov (KS) test was used to evaluate whether the high-income tail of the USA household income distribution is consistent with a power-law distribution (Eq 17) or with an exponential distribution (Eq 18). The term “theoretical distribution” is used below to refer to the distribution (either power-law or exponential) that the real data is compared to in the statistical test.

The KS test relies on the “KS distance”, which is the largest distance between the cumulative distribution function (CDF) of the theoretical distribution (with specified parameters) and the empirical cumulative distribution function, F_N , determined directly from the data as follows:

$$F_N(x) = \frac{1}{N} \sum_{i=1}^N I_{[-\infty, x]}(X_i), \quad (19)$$

where $I_{[-\infty, x]}(X_i)$ is the indicator function, which is equal to 1 if $X_i \leq x$ and 0 otherwise, and N is the number of data points in the dataset. The 2015 USA household income dataset is a weighted dataset, such that every data point represents a particular number of people in the overall population. For this dataset, the weighted empirical cumulative distribution function [50] was used:

$$F_w(x) = \frac{1}{\sum_i w_i} \sum_{i=1}^N w_i I_{[-\infty, x]}(X_i), \quad (20)$$

where w_i is the weight assigned to the i_{th} data point.

Since the parameters γ (power-law distribution) and T (exponential distribution) are unknown, they are estimated from the data using maximum likelihood estimation for the unweighted 2000 dataset and weighted maximum likelihood estimation for the 2015 dataset [51].

The KS distance, D_{data} , between the empirical CDF (F_N or F_w) and the CDF of the theoretical distribution is compared to a distribution of KS distances determined from synthetic datasets. To obtain the latter distribution of KS distances, the following steps are repeated many times: 1) a sample of synthetic data containing the same number of data points as the real data is drawn from the theoretical distribution; 2) the parameters of the theoretical distribution are re-estimated from the synthetic data, in order to avoid biases that arise if this re-estimation is not performed [52]; 3) the KS distance, D_{synth} , is determined from the empirical CDF of the synthetic data and the theoretical distribution with re-estimated parameters.

If the real data is consistent with the theoretical distribution, D_{data} should be smaller than a significant fraction of the set of $\{D_{synth}\}$. The fraction of $\{D_{synth}\}$ that is larger than D_{data} is the p -value given by the test. We consider a p -value greater than 0.1 to be evidence of compatibility with the theoretical distribution. In other words, with a p -value greater than 0.1, there is not enough evidence to reject the null hypothesis that the real data comes from the theoretical distribution.

A KS test showed that the high-income tail of the 2015 USA household income data is only compatible (p -value > 0.1) with an exponential distribution within particular ranges $[S_l, S_h]$ within the high-income tail, the largest of which is \$700,000 to \$1,700,000 (\$492,800 to \$1,196,800 in 1999 USD), and that the high-income tail is not compatible with a power-law for any of the ranges tested. The KS test for the 2000 USA household data also shows that the data is only compatible with an exponential distribution within particular ranges, the largest being from \$800,000 to the largest income value in the dataset (\$1,668,400), and that the high-income tail is not compatible with a power-law for any of the ranges tested.

S2.C Alternative “extended” models that pre-suppose a two-class structure

S2.C.1 Addition to extended model to allow fights between high-status individuals

In the extended model presented in section 2.1 of the main text, individuals at the top-end of the status distribution are separated by large amounts of status, typically greater than the amount $\eta\bar{S}$. These high-status individuals are therefore prevented from fighting with each other by the first condition ($S_1 - S_2 > \eta\bar{S}$) of the extended model. This excludes many fights between high-status “dominant” individuals and higher-than-average status “challengers”, whereas such dominant-challenger fights are important and common in real dominance hierarchies [30–32]. In order to allow high-status individuals to fight each other more frequently, we introduce a third condition to the extended model, such that the fight occurs if the statuses of both potential competitors are greater than the threshold amount $\eta\bar{S}$ (equivalently, if $S_2 > \eta\bar{S}$, since $S_1 \geq S_2$). Under this modification to the extended model, the fight occurs if $S_1 - S_2 \leq \eta\bar{S}$ OR $S_2 > \eta\bar{S}$ OR $r \leq \epsilon$, where r is a random number between 0 and 1. The additional condition $S_2 > \eta\bar{S}$, pre-supposes a two-class structure *a priori*. The status distributions produced by this 3-condition extended model have large- S tails that decay exponentially over the full extent of the tail, unlike those produced by the 2-condition extended model presented in section 2.1 of the main text, which show a cutoff at very high values of S (see Fig 12f of the main text). The status distributions of the 3-condition model therefore show improved fits to the proxy data, as can be seen in Fig 37.

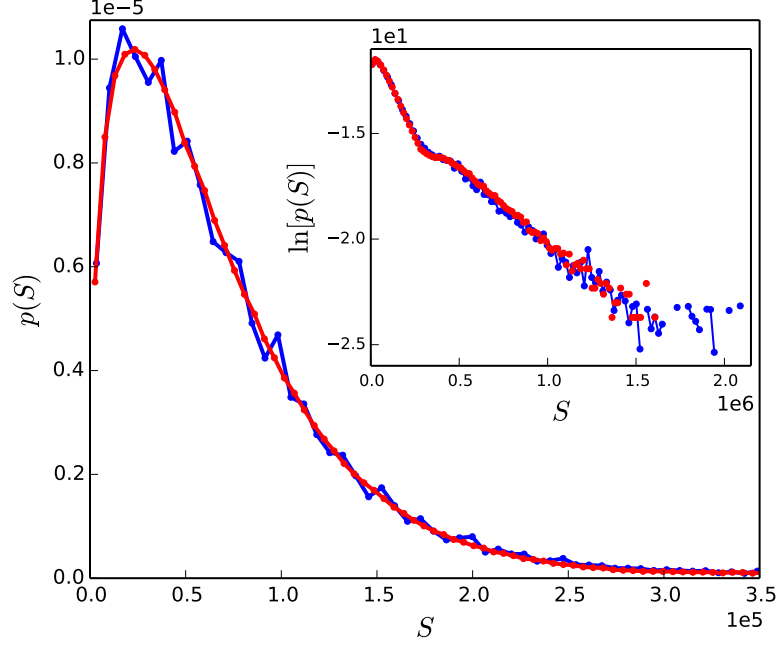


Fig 37: Fit of 3-condition extended model status distribution (red curve) to the 2015 USA household income distribution (blue curve). Simulation parameters: $\delta = 0.4$, $\alpha = 0$, $\eta = 3.5$, $\epsilon = 0.08$.

S2.C.2 Combining two independently simulated status distributions

Here, we have used the original (two-parameter) model presented in section 2 of the main text and simulated two separate populations with different N and \bar{S} . The combination of the two simulated status distribution provides a good fit to the American household income distribution. This is shown in Fig 38, where the blue curve is the American household income distribution data for the year 2015, the red and green curves represent the two independently-simulated status distributions, and the cyan curve shows the combination of the two simulated distributions. The simulation that produced the green curve contained $N_1 = 0.1N_{dat}$ individuals, where $N_{dat} = 1,226,728$ is the number of households in the dataset. For this first simulated society, $\bar{S}_1 = 225,000$. The simulation that produced the red curve contained $N_2 = 0.9N_{dat}$ individuals with $\bar{S}_2 = 64,445$. \bar{S}_1 and \bar{S}_2 were chosen so that the total status of the two simulated systems $\bar{S}_1 N_1 + \bar{S}_2 N_2$ was equal to the total household income reported in the dataset.

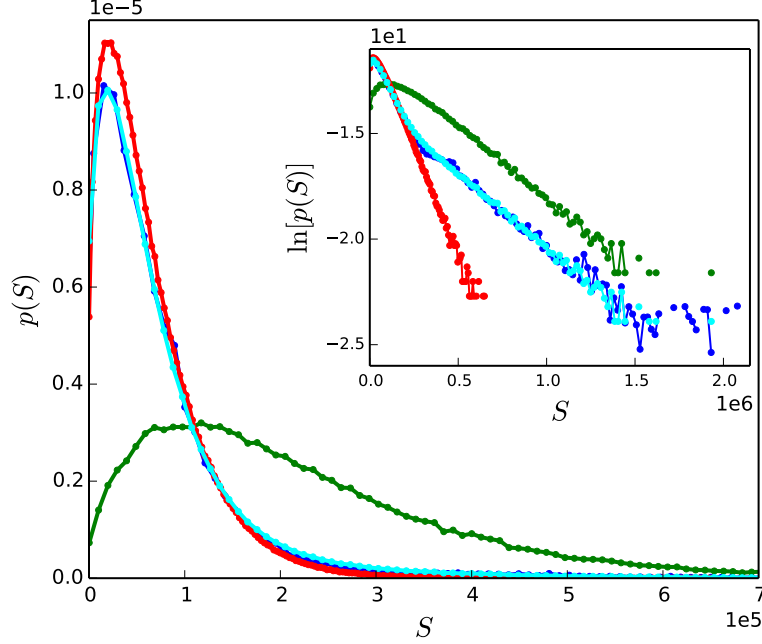


Fig 38: Fit of simulated distribution to USA data. Cyan curve is the combination of red and green distributions. For red curve, $N = 0.9N_{dat}$, $\bar{S} = 64,445$, and $\delta = 0.4$; for green curve, $N = 0.1N_{dat}$, $\bar{S} = 225,000$, and $\delta = 0.35$. $\alpha = 0$ for both red and green curves.

As shown in Fig 38, the American household income data is well-represented by the combination of the status distributions of (i) a simulated system with a relatively small number of individuals having a relatively high average status, and (ii) a simulated system with a relatively large number of individuals having a relatively modest average status. This approach differs from those presented in sections 2.1 of the main text and section S2.C.1, by assuming that the society consists of two separate groups for which the members of each group engage in status-determining interactions amongst themselves, but for which there are no cross-group interactions. The extended model presented in section 2.1 of the main text makes no such assumptions.

References

1. Sapolsky RM. The Influence of Social Hierarchy on Primate Health. *Science*. 2005;308(5722):648–652. doi:10.1126/science.1106477.
2. Boyce WT. Social stratification, health, and violence in the very young. *Annals of the New York Academy of Sciences*. 2004;1036:47–68. doi:10.1196/annals.1330.003.
3. Jensen K. Punishment and spite, the dark side of cooperation. *Philosophical Transactions of the Royal Society B: Biological Sciences*. 2010;365(1553):2635–2650. doi:10.1098/rstb.2010.0146.
4. Choi JK, Bowles S. The Coevolution of Parochial Altruism and War. *Science*. 2007;318(5850):636–640.
5. Shayo M. A Model of Social Identity with an Application to Political Economy: Nation, Class, and Redistribution. *American Political Science Review*. 2009;103(02):147–174. doi:10.1017/S0003055409090194.
6. Lindquist WB, Chase ID. Data-based analysis of winner-loser models of hierarchy formation in animals. *Bulletin of Mathematical Biology*. 2009;71(3):556–584. doi:10.1007/s11538-008-9371-9.
7. Yakovenko VM, Rosser JB. Colloquium: Statistical mechanics of money, wealth, and income. *Reviews of Modern Physics*. 2009;81(4):1703–1725. doi:10.1103/RevModPhys.81.1703.
8. Kunst JR, Fischer R, Sidanius J, Thomsen L. Preferences for group dominance track and mediate the effects of macro-level social inequality and violence across societies. *Proceedings of the National Academy of Sciences*. 2017;114(21):5407–5412. doi:10.1073/pnas.1616572114.
9. Hobbes T. *Leviathan*. Oxford University Press; 1998.
10. Lagasse P. Marxism. In: *The Columbia Encyclopedia*. 7th ed. Columbia University Press; 2017.
11. Butzer KW. Collapse, environment, and society. *Proceedings of the National Academy of Sciences*. 2012;109(10):3632–3639. doi:10.1073/pnas.1114845109.
12. Diamond J. Two views of collapse. *Nature*. 2010;463(February):880–882. doi:10.1038/463880a.
13. Rand DG, Nowak MA. Human cooperation. *Trends in Cognitive Sciences*. 2013;17(8):413–425. doi:10.1016/j.tics.2013.06.003.
14. Fehr E, Fischbacher U. Social norms and human cooperation. *Trends in Cognitive Sciences*. 2004;8(4):185–190. doi:10.1016/j.tics.2004.02.007.

15. Chase ID, Tovey C, Spangler-Martin D, Manfredonia M. Individual differences versus social dynamics in the formation of animal dominance hierarchies. *Proceedings of the National Academy of Sciences of the United States of America*. 2002;99(8):5744–5749.
16. Franz M, McLean E, Tung J, Altmann J, Alberts SC. Self-organizing dominance hierarchies in a wild primate population. *Proceedings of the Royal Society B: Biological Sciences*. 2015;282(1814):20151512. doi:10.1098/rspb.2015.1512.
17. Bonabeau E, Theraulaz G, Deneubourg JL. Phase diagram of a model of self-organizing hierarchies. *Physica A: Statistical Mechanics and its Applications*. 1995;217(3-4):373–392. doi:10.1016/0378-4371(95)00064-E.
18. Ben-Naim E, Redner S. Dynamics of social diversity. *Journal of Statistical Mechanics: Theory and Experiment*. 2005;11002(11):9–16. doi:10.1088/1742-5468/2005/11/L11002.
19. Ben-Naim E, Vazquez F, Redner S. On the structure of competitive societies. *European Physical Journal B*. 2006;49(4):531–538. doi:10.1140/epjb/e2006-00095-y.
20. Dugatkin LA. Winner and loser effects and the structure of dominance hierarchies. *Behavioral Ecology*. 1997;8(6):583–587. doi:10.1093/beheco/8.6.583.
21. Hemelrijk CK. An individual-orientated model of the emergence of despotic and egalitarian societies. *Proceedings of the Royal Society B: Biological Sciences*. 1999;266(1417):361–369. doi:10.1098/rspb.1999.0646.
22. Hemelrijk CK. Towards the integration of social dominance and spatial structure. *Animal Behaviour*. 2000;59(5):1035–1048. doi:10.1006/anbe.2000.1400.
23. Ispolatov S, Krapivsky PL, Redner S. Wealth distributions in asset exchange models. *The European Physical Journal B*. 1998;2:267–276. doi:10.1007/s100510050249.
24. Hayes B. Follow The Money. *American Scientist*. 2002;90(5):400–405.
25. Boghosian BM, Johnson M, Marcq JA. An H Theorem for Boltzmann’s Equation for the Yard-Sale Model of Asset Exchange: The Gini Coefficient as an H Functional. *Journal of Statistical Physics*. 2015;161(6):1339–1350. doi:10.1007/s10955-015-1316-8.
26. Chakraborti A, Toke IM, Patriarca M, Abergel F. Econophysics review: II. Agent-based models. *Quantitative Finance*. 2011;11(January):1013. doi:10.1080/14697688.2010.539249.
27. Boghosian BM, Devitt-Lee A, Johnson M, Li J, Marcq JA, Wang H. Oligarchy as a phase transition: The effect of wealth-attained advantage in a FokkerPlanck description of asset exchange. *Physica A: Statistical Mechanics and its Applications*. 2017;476:15–37. doi:10.1016/j.physa.2017.01.071.

28. Boghosian BM, Devitt-Lee A, Li J, Marcq JA, Wang H. Describing Realistic Wealth Distributions with the Extended Yard-Sale Model of Asset Exchange. 2016; Preprint. Available from: [arXiv:1604.02370](https://arxiv.org/abs/1604.02370).
29. Boghosian BM, Devitt-Lee A, Wang H. The Growth of Oligarchy in a Yard-Sale Model of Asset Exchange: A Logistic Equation for Wealth Condensation. In: 1st International Conference on Complex Information Systems; 2016. doi:10.5220/0005956501870193.
30. Sapolsky RM. Cortisol concentrations and the social significance of rank instability among wild baboons. *Psychoneuroendocrinology*. 1992;17(6):701–709. doi:10.1016/0306-4530(92)90029-7.
31. Gesquiere LR, Learn NH, Simao MCM, Onyango PO, Alberts SC, Altmann J. Life at the Top: Rank and Stress in Wild Male Baboons. *Science*. 2011;333(6040):357–360. doi:10.1126/science.1207120.
32. Sapolsky RM. Sympathy for the CEO. *Science*. 2011;333(6040):293–294. doi:10.1126/science.1209620.
33. Côté S, Kraus MW, Carpenter NC, Piff PK, Beermann U, Keltner D. Social affiliation in same-class and cross-class interactions. *Journal of Experimental Psychology: General*. 2017;146(2):269–285.
34. Massey DS, Denton NA. *American apartheid: segregation and the making of the underclass*. Harvard University Press; 1993.
35. Silk JB. Practice Random Acts of Aggression and Senseless Acts of Intimidation: The Logic of Status Contests in Social Groups. *Evolutionary Anthropology*. 2002;11(6):221–225. doi:10.1002/evan.10038.
36. Hänggi P, Talkner P, Borkovec M. Reaction-rate theory: Fifty years after Kramers. *Reviews of Modern Physics*. 1990;62(2):251–341. doi:10.1103/RevModPhys.62.251.
37. Markov IV. *Crystal growth for beginners*. 2nd ed. World Scientific Publishing; 2003.
38. Angell CA. Relaxation on liquid, polymers and plastic crystal - strong/fragile patterns and problems. *Journal of Non-Crystalline Solids*. 1991;131-133:13–31.
39. Knobel M, Nunes WC, Socolovsky LM, De Biasi E, Vargas JM, Denardin JC. Superparamagnetism and Other Magnetic Features in Granular Materials: A Review on Ideal and Real Systems. *Journal of Nanoscience and Nanotechnology*. 2008;8:2836–2857.
40. Laidler KJ. Unconventional applications of the Arrhenius law. *Journal of Chemical Education*. 1972;49(5):343. doi:10.1021/ed049p343.
41. Shavers VL. Measurement of socioeconomic status in health disparities research. *Journal of the National Medical Association*. 2007;99(9):1013–23.

42. Statistics Canada. Census of Canada, 2001: public use microdata file - households and housing file [computer file]. Phase 2 release. Ottawa, Ont. Data Liberation Initiative [distributor], 2006/06/30. (STC 95M0020XCB).
43. Chakrabarti AS, Chakrabarti BK. Statistical Theories of Income and Wealth Distribution. *Economics: The Open-Access, Open-Assessment E-Journal*. 2010;4:1–32. doi:10.5018/economics-ejournal.ja.2010-4.
44. Statistics Canada 2001 Census Public Use Microdata File: Households and housing file user documentation. Ottawa, Ont. Data Liberation Initiative [distributor], 2006/06/30. (STC 95M0020XCB).
45. Ruggles S, Genadek K, Goeken R, Grover J, Sobek M. Integrated Public Use Microdata Series: Version 6.0 [dataset]. Minneapolis: University of Minnesota, 2015. doi:10.18128/D010.V6.0.
46. Ruggles S, Genadek K, Goeken R, Grover J, Sobek M. Note on Adjusting Dollar Amount Variables for Inflation. IPUMS USA, University of Minnesota; 2017. Available from: <https://usa.ipums.org/usa/cpi99.shtml>.
47. Slanina F. Essentials of econophysics modelling. Oxford University Press; 2013.
48. Richmond P, Mimkes J, Hutzler S. Econophysics and physical economics. Oxford Scholarship Online; 2013.
49. Baró J, Vives E. Analysis of power-law exponents by maximum-likelihood maps. *Physical Review E*. 2012;85:066121. doi:10.1103/PhysRevE.85.066121.
50. SAS Institute Inc. SAS/INSIGHT User's Guide. SAS Online Doc, Version 8. 2000. Available from: <http://www.okstate.edu/sas/>.
51. Wang SX. Maximum weighted likelihood estimation. PhD thesis, University of British Columbia. 2001. doi:10.14288/1.0090880.
52. Capasso M, Alessi L, Barigozzi M, Fagiolo G. On approximating the distributions of goodness-of-fit test statistics based on the empirical distribution function: The case of unknown parameters. *Advances in Complex Systems*. 2009;12(2):157. doi:10.1142/S0219525909002131.
53. Flinn MV, Ponzi D, Muehlenbein MP. Hormonal Mechanisms for Regulation of Aggression in Human Coalitions. *Human Nature*. 2012;23(1):68–88. doi:10.1007/s12110-012-9135-y.
54. Wilson ML, Wrangham RW. Intergroup Relations in Chimpanzees. *Annual Review of Anthropology*. 2003;32(1):363–392. doi:10.1146/annurev.anthro.32.061002.120046.
55. Hemelrijk CK, Kappeler PM, Puga-Gonzalez I. The Self-organization of Social Complexity in Group-Living Animals: Lessons From the DomWorld Model. *Advances in the Study of Behavior*. 2017;49:361-405. doi: 10.1016/bs.asb.2017.02.005.

56. Leymann H. The content and development of mobbing at work. *European Journal of Work and Organizational Psychology*. 1996;5(2):165–184. doi:10.1080/13594329608414853.
57. Graw B, Manser MB. The function of mobbing in cooperative meerkats. *Animal Behaviour*. 2007;74(3):507–517. doi:10.1016/j.anbehav.2006.11.021.